

A Brief History of Astrodynamics

Ancients to 1543

Nicolaus Copernicus, 1543

Galileo Galilei, 1632

Tycho Brahe, 1546-1601

Johannes Kepler, 1619

Isaac Newton, 1687

Albert Einstein, 1920

.

Geocentric Universe

"Revolutions of the Celestial Sphere"

"Dialogue on the Two Chief Systems of the World, the Ptolemaic and Copernican"

Rudolphine Tables

"New Astronomy" (2nd Law)

"Harmony of the Worlds" (3rd Law)

"Law of Universal Gravitation,"

$F=GMm/r^2$

Three Laws of Motion

Relativity: the special

and general theory

This nose is licensed under the Creative Commons Attribution-Share Alike 2.0 Generic license.



≡ 3.1 - Kepler & Newton

Module 3: Orbits & Signals

GNSS Orbits

3.1 Brahe, Kepler & Newton

3.2 Coordinate frames

3.3 Transforming from Keplerian parameters to ECEF

3.4 Decoding the GPS navigation message

GNSS Signals

3.5 L band

3.6 Frequency domain

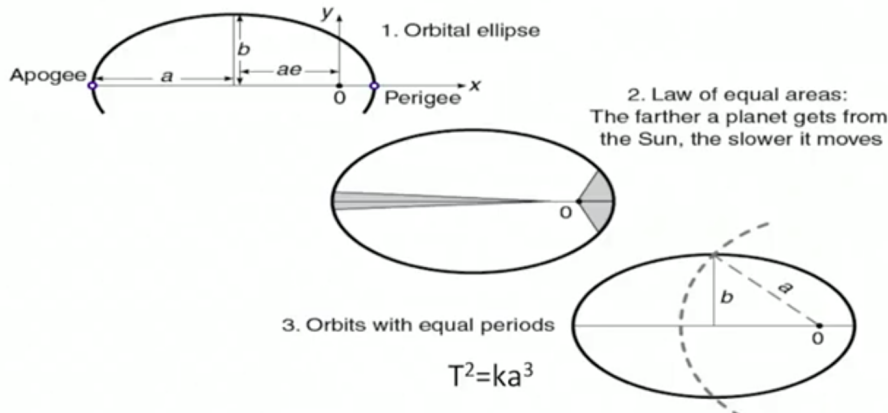
3.7 Amplitude spectra of GNSS signals

3.8 Auto-correlation & Cross-correlation

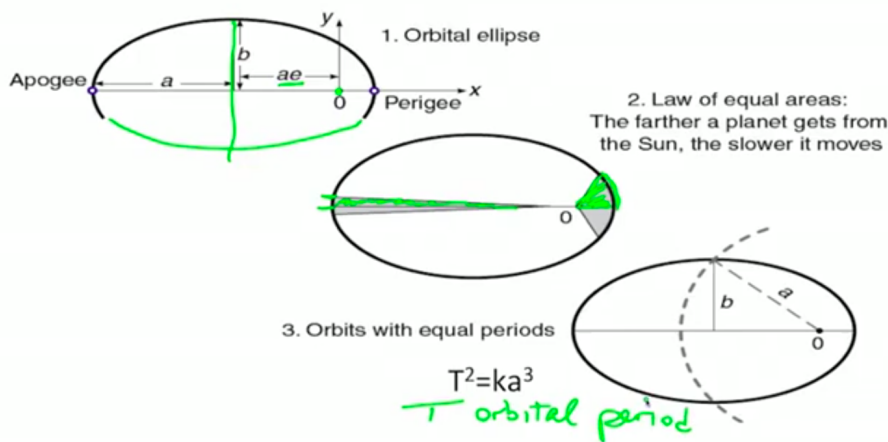
3.9 New GNSS signals



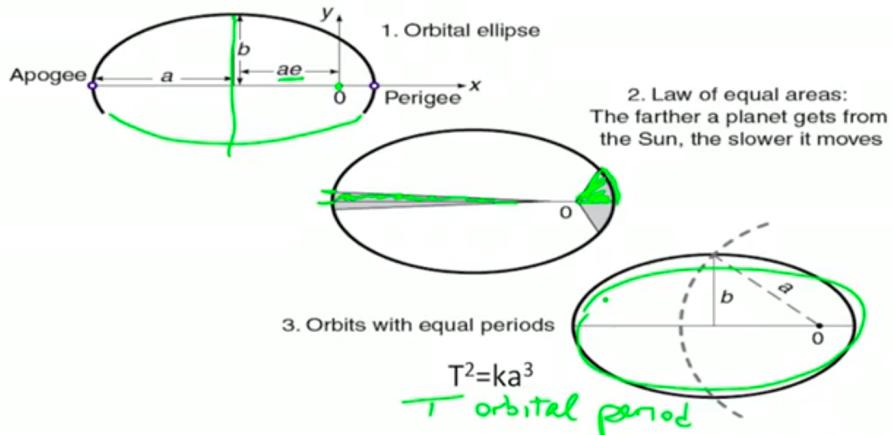
Kepler's Three Laws Illustrated



Kepler's Three Laws Illustrated



Kepler's Three Laws Illustrated



Fundamental Orbital Differential Equation (FODE)

$$\underline{E}_{G,n} = -Gm_n \sum_{\substack{j=1 \\ j \neq n}}^J \frac{-m_j \underline{r}_{j,n}}{\underline{r}_{j,n}^3}$$

$$\ddot{\underline{r}}_n = -G \sum_{\substack{j=1 \\ j \neq n}}^J \frac{-m_j \underline{r}_{j,n}}{\underline{r}_{j,n}^3}$$

$$\ddot{\underline{r}}_n = \frac{-G(m_1 + m_2) \underline{r}_{1,2}}{\underline{r}_{1,2}^3} - G \sum_{j=3}^J m_j \left(\frac{\underline{r}_{j,2}}{\underline{r}_{j,2}^3} - \frac{\underline{r}_{j,1}}{\underline{r}_{j,1}^3} \right)$$

$$\ddot{\underline{r}}_{1,2} = \frac{-G(M+m) \underline{r}_{1,2}}{\underline{r}_{1,2}^3}$$

$$M_E = 6 \times 10^{24} \text{ kg}$$

$$m_{SV} = 10^3 \text{ kg}$$

$$\ddot{\underline{r}} + \frac{GM}{r^2} \frac{\underline{r}}{r} = 0$$

$$G = 6,673 \times 10^{-11} \text{ kg}^{-1} / \text{s}^2$$

$$GM = \mu = 3.986005 \times 10^{14} \text{ m}^3 / \text{s}^2$$

$$\ddot{\underline{r}} + \frac{\mu \underline{r}}{r^3} = 0$$



Fundamental Orbital Differential Equation (FODE)

$$\underline{E}_{G,n} = -Gm_n \sum_{\substack{j=1 \\ j \neq n}}^J \frac{-m_j \underline{r}_{j,n}}{\underline{r}_{j,n}^3}$$

$$\ddot{\underline{r}}_n = -G \sum_{\substack{j=1 \\ j \neq n}}^J \frac{-m_j \underline{r}_{j,n}}{\underline{r}_{j,n}^3}$$

$$\ddot{\underline{r}}_n = \frac{-G(m_1 + m_2) \underline{r}_{1,2}}{\underline{r}_{1,2}^3} - G \sum_{j=3}^J m_j \left(\frac{\underline{r}_{j,2}}{\underline{r}_{j,2}^3} - \frac{\underline{r}_{j,1}}{\underline{r}_{j,1}^3} \right)$$

$$\ddot{\underline{r}}_{1,2} = \frac{-G(M+m) \underline{r}_{1,2}}{\underline{r}_{1,2}^3}$$

$$M_E = 6 \times 10^{24} \text{ kg}$$

$$m_{SV} = 10^3 \text{ kg}$$

$$\ddot{\underline{r}} + \frac{GM}{r^2} \frac{\underline{r}}{r} = 0$$

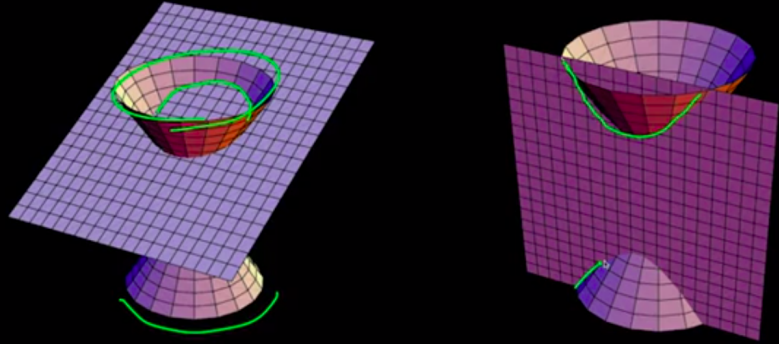
$$G = 6,673 \times 10^{-11} \text{ kg}^{-1} / \text{s}^2$$

$$GM = \mu = 3.986005 \times 10^{14} \text{ m}^3 / \text{s}^2$$

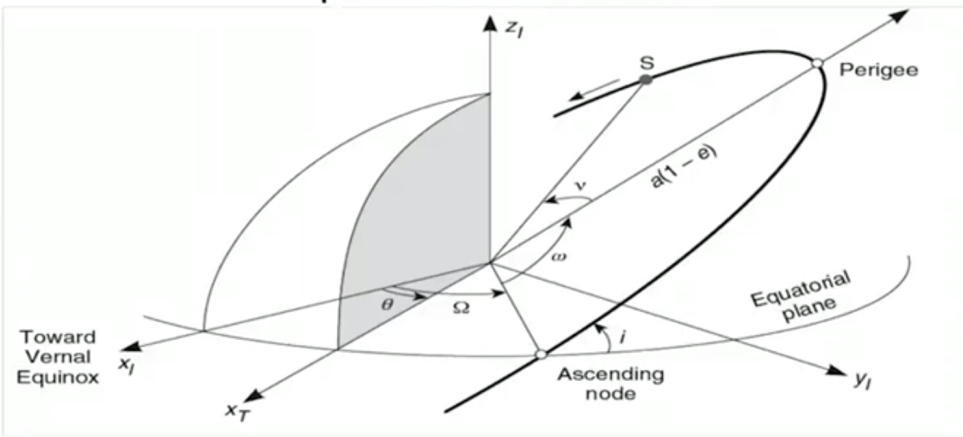
$$\ddot{\underline{r}} + \frac{\mu \underline{r}}{r^3} = 0$$



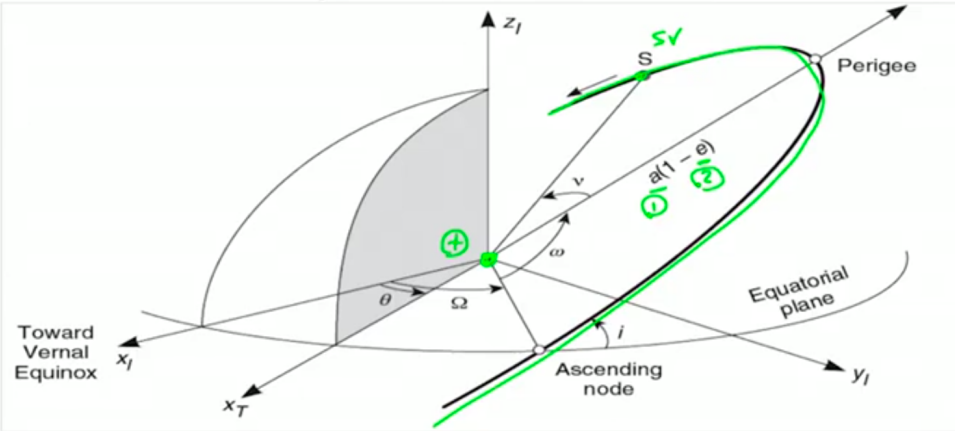
Conic Sections



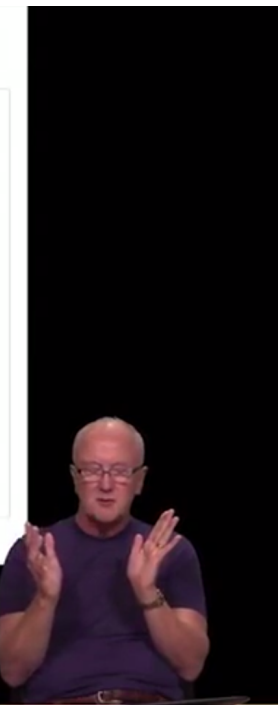
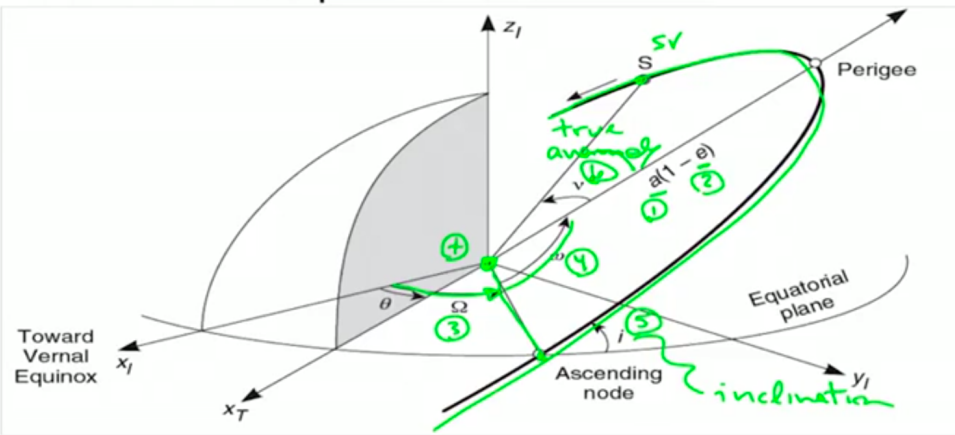
Keplerian Parameters



Keplerian Parameters



Keplerian Parameters



Coordinate Frames Introduced

- Helio-centric
- Geo-centric
 - Earth centered inertial (ECI, IJK)
 - Perifocal (also inertial)
 - Earth centered earth-fixed (ECEF)
 - Sidereal (versus solar) time
 - Right ascension of the ascending node (RAAN)
 - Longitude of the ascending node (LAN)
- User-centric
 - Topocentric, horizon (SEZ, NED)

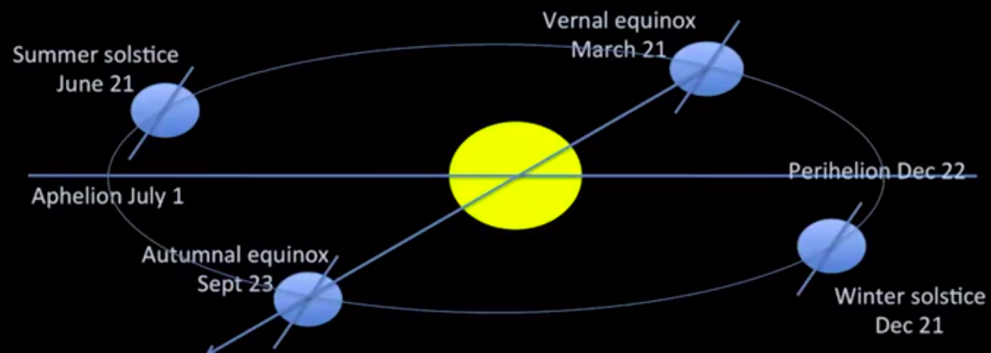


Coordinate Frames Introduced

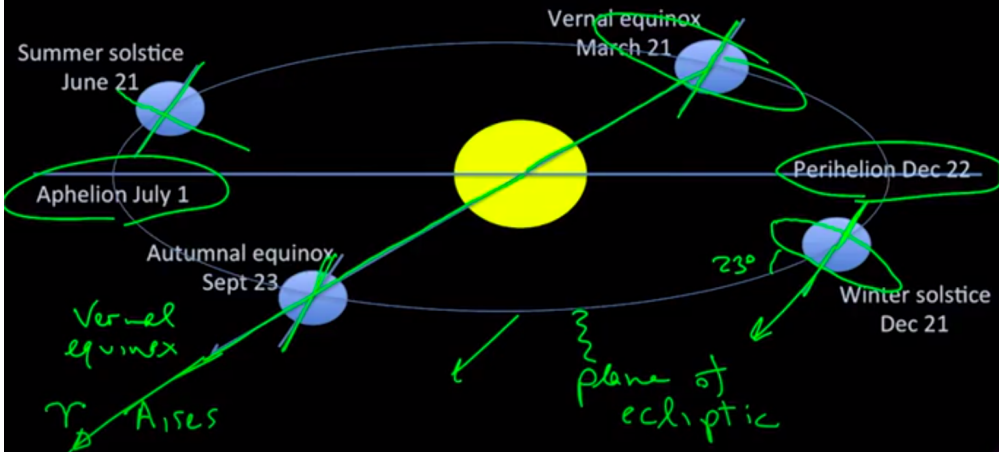
- Most GNSS orbit calculation are transformations from one frame to another
- Keplerian parameters →
 - Peri-focal coordinates →
 - Earth-centered inertial →
 - Earth-centered earth-fixed



Heliocentric Reference Frame



Heliocentric Reference Frame



◀ ▶ ⏪ 8:56 / 11:06

Scroll for details



Three Definitions of Vernal Equinox

T-Series
www.youtube.com
It's My Life Song (Full Song)|Harman Baweja, Genelia D'Souza, Nana Patekar|Mika Singh, Shankar-Ehsaan-Loy

Settings

Summer solstice June 21

Vernal equinox, March 21
tilt of Earth's axis neither points toward or away from Sun

Aphelion July 1

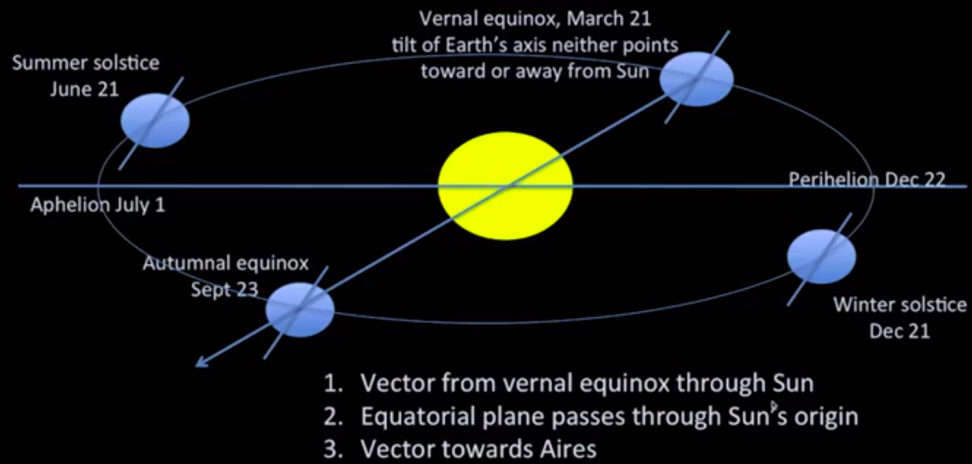
Autumnal equinox Sept 23

Perihelion Dec 22

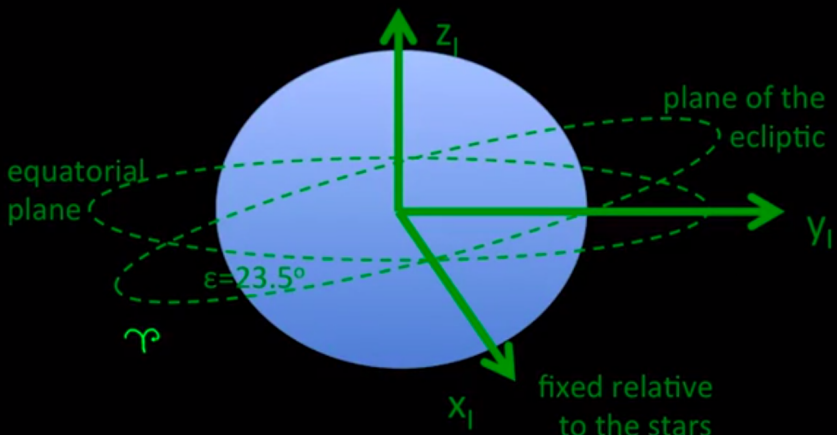
Winter solstice Dec 21

1. Vector from vernal equinox through Sun
2. Equatorial plane passes through Sun's origin
3. Vector towards Aires

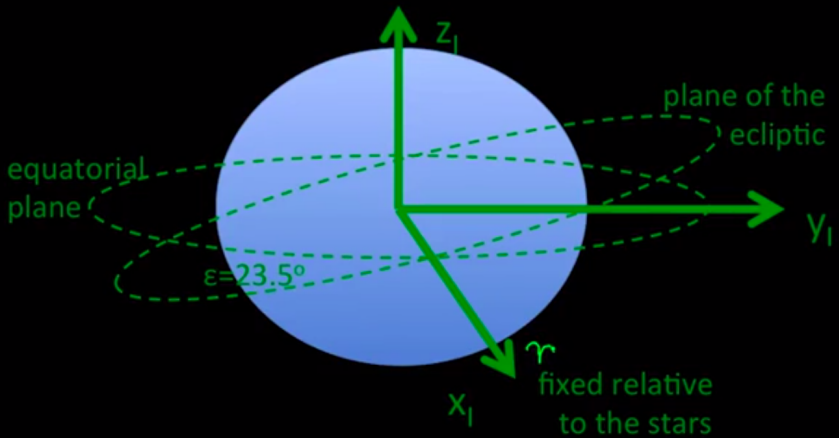
Three Definitions of Vernal Equinox



Earth Centered Inertial (I,J,K)



Earth Centered Inertial (I,J,K)



Module 3: Orbits & Signals

GNSS Orbits

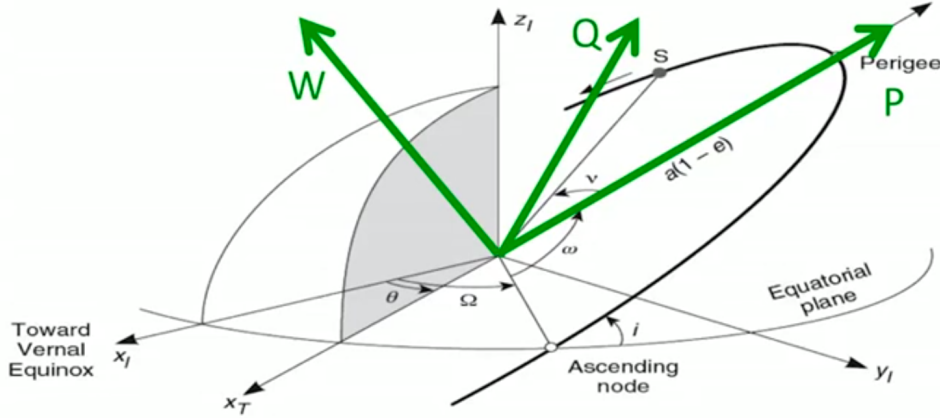
- 3.1 Brahe, Kepler & Newton
- 3.2 Coordinate frames
- 3.3 Transforming from Keplerian parameters to ECEF
- 3.4 Decoding the GPS navigation message

GNSS Signals

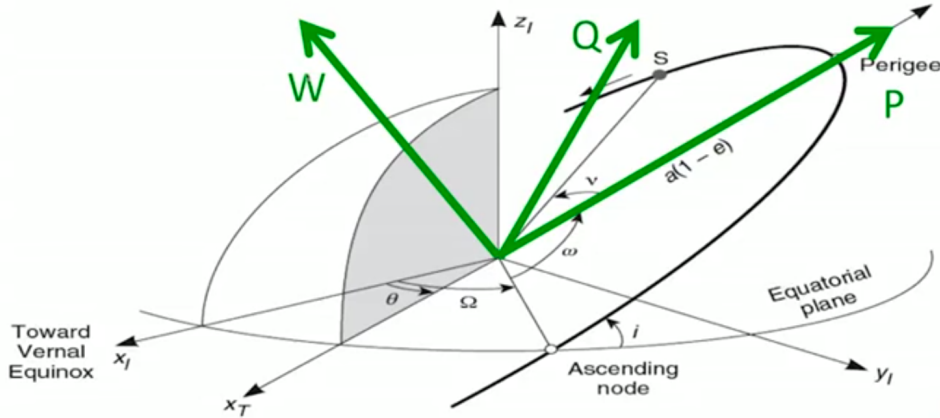
- 3.5 L band
- 3.6 Frequency domain
- 3.7 Amplitude spectra of GNSS signals
- 3.8 Auto-correlation & Cross-correlation
- 3.9 New GNSS signals



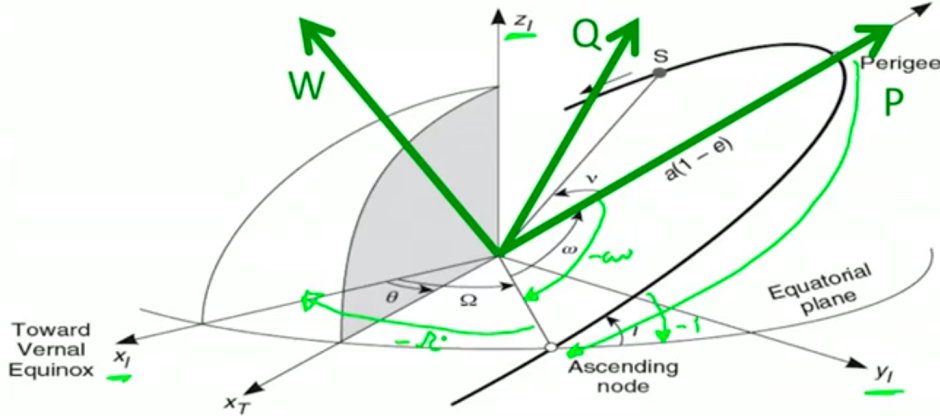
Perifocal Reference System



Perifocal Reference System



Perifocal Reference System



from Keplerian $\{a, e, \Omega, \omega, \dot{\Omega}, \dot{\omega}\}$
 to Perifocal $\{\Sigma\}_{PQW}$
 to ECI $\{\Sigma\}_{ECT}$

$$\Sigma_{PQW} = \frac{a(1-e^2)}{1+e\cos\Omega} \begin{bmatrix} \cos\Omega \\ \sin\Omega \\ 0 \end{bmatrix}$$

$$\Sigma_{PQW} = r \cos\Omega \mathbf{P} + r \sin\Omega \mathbf{Q} + \mathbf{O}$$

By the way,

$$\begin{aligned} \Sigma_{PQW} &= \Sigma_{PQW} && \text{eccentricity} \\ &= -\sqrt{\frac{GM}{r}} \sin\Omega \mathbf{P} + \sqrt{\frac{GM}{r}} (e + \cos\Omega) \mathbf{Q} + \mathbf{O} && \text{perihelion radius} \end{aligned}$$

$$\Sigma_{ECI} = \text{Rot}_3[-\Omega] \text{Rot}_1[-i] \text{Rot}_3[\omega] \Sigma_{PQW}$$

$$\Sigma_{ECI} = (\text{Rot}_3[-\Omega] \text{Rot}_1[-i] \text{Rot}_3[\omega]) \Sigma_{PQW}$$



from Keplerian $\{a, e, i, \Omega, \omega, D_0\}$
 to Perifocal $\{\underline{\Sigma}\}_{\text{POW}}$
 to ECI $\{\underline{\Sigma}\}_{\text{ECT}}$

$$\underline{\Sigma}_{\text{POW}} = \frac{a(1-e^2)}{1+e\cos\Omega} \begin{bmatrix} \cos\Omega \\ \sin\Omega \\ 0 \end{bmatrix}$$

$$\underline{\Sigma}_{\text{POW}} = r \cos\Omega \underline{\hat{P}} + r \sin\Omega \underline{\hat{Q}} + \underline{\hat{O}}$$

By the way,

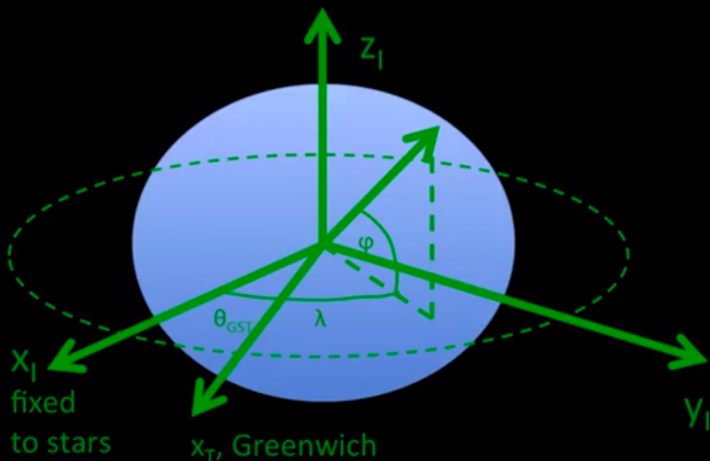
$$\begin{aligned} \underline{\Sigma}_{\text{POW}} &= \underline{\Sigma}_{\text{POW}} \\ &= -\sqrt{\frac{GM}{r}} \sin\Omega \underline{\hat{P}} + \sqrt{\frac{GM}{r}} (e + \cos\Omega) \underline{\hat{Q}} + \underline{\hat{O}} \end{aligned} \quad \begin{matrix} \text{eccentricity} \\ \text{per semi-latus} \end{matrix}$$

$$\underline{\Sigma}_{\text{ECT}} = \text{Rot}_3[-\alpha] \text{Rot}_1[-i] \text{Rot}_3[-\omega] \underline{\Sigma}_{\text{POW}}$$

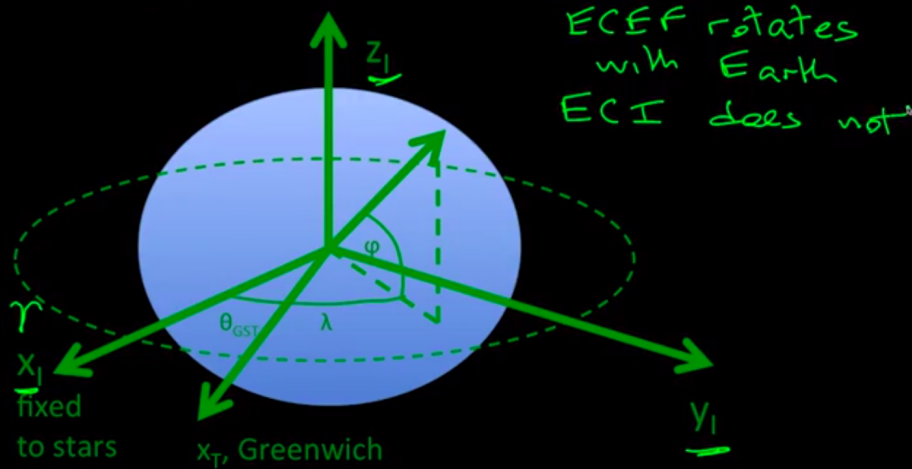
$$\underline{\Sigma}_{\text{ECT}} = \text{Rot}_3[-\alpha] \text{Rot}_1[-i] \text{Rot}_3[-\omega] \underline{\Sigma}_{\text{POW}}$$



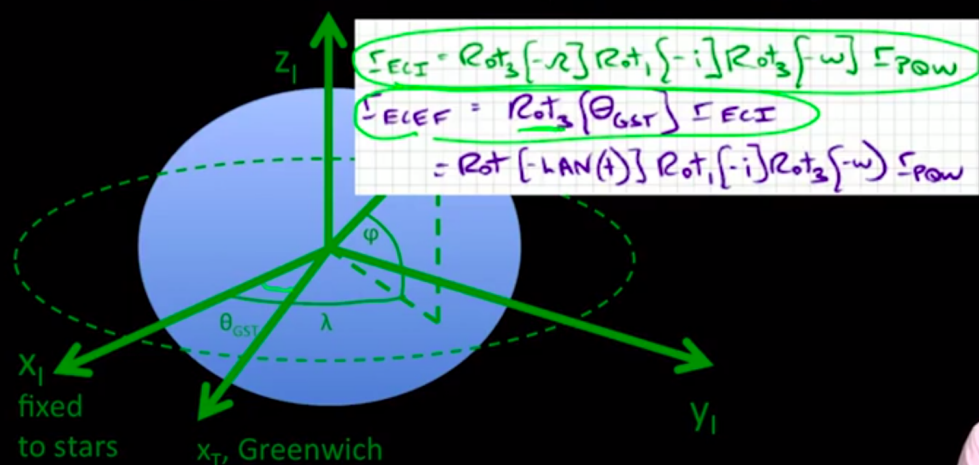
Earth Centered Earth Fixed (ECEF)



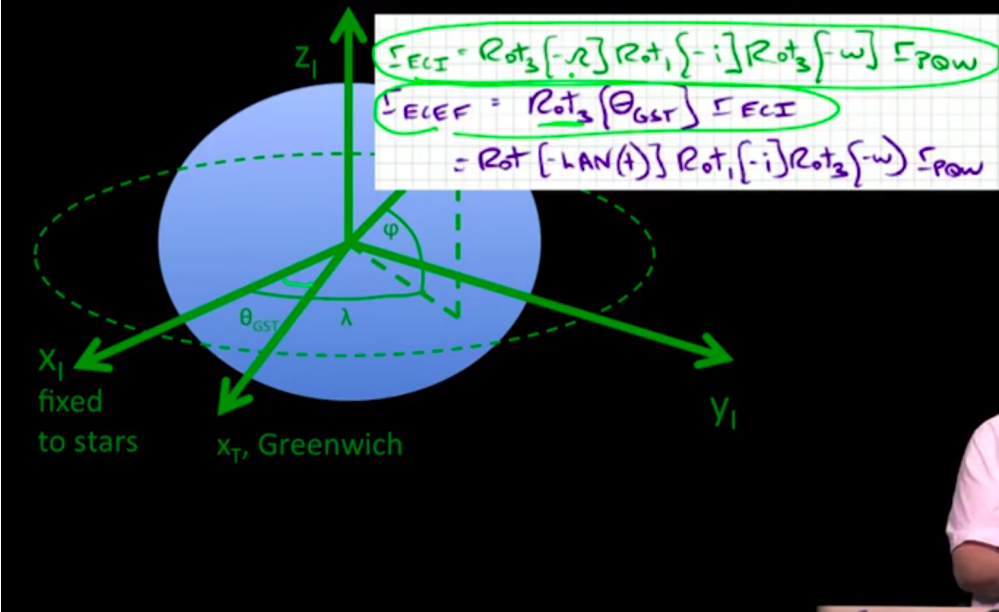
Earth Centered Earth Fixed (ECEF)



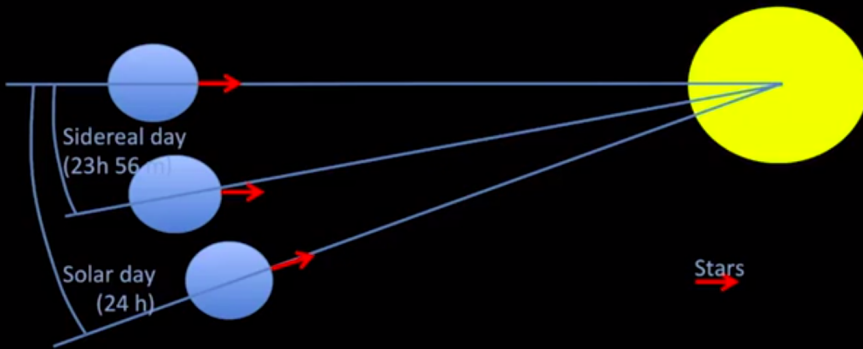
Earth Centered Earth Fixed (ECEF)



Earth Centered Earth Fixed (ECEF)



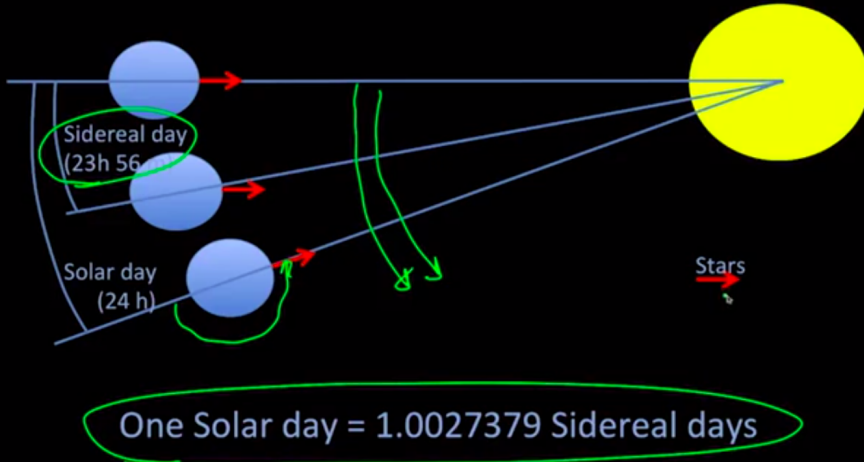
Sidereal and Solar Time



One Solar day = 1.0027379 Sidereal days



Sidereal and Solar Time



Anomalies (Angles)

True anomaly, v

Eccentric anomaly, E

Mean anomaly, M

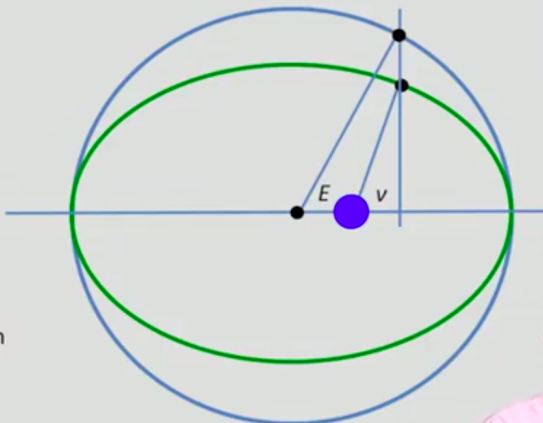
$$T = \frac{2\pi}{\sqrt{\mu}} a^{3/2} \quad \text{orbital period}$$

$$n = \frac{2\pi}{T} = \sqrt{\frac{\mu}{a^3}} \quad \text{mean motion}$$

$$M = M_0 + n(t - t_p) \quad \text{mean anomaly}$$

$$M = E - e \sin E \quad \text{Keplers equation}$$

$$v = \tan^{-1} \left(\frac{\sqrt{1-e^2} \sin E}{\cos E - e} \right)$$



Anomalies (Angles)

True anomaly, v

Eccentric anomaly, E

Mean anomaly, M

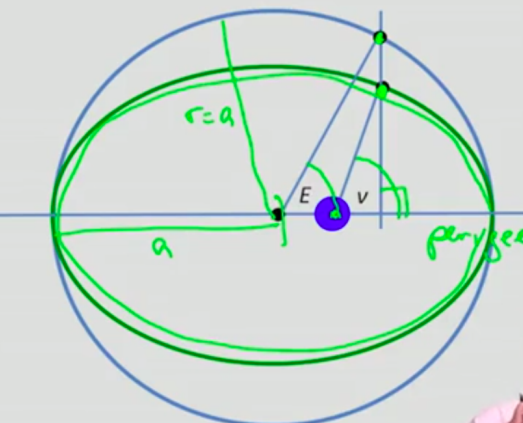
$$T = \frac{2\pi}{\sqrt{\mu}} a^{3/2} \quad \text{orbital period}$$

$$n = \frac{2\pi}{T} = \sqrt{\frac{\mu}{a^3}} \quad \text{mean motion}$$

$$M = M_0 + n(t - t_p) \quad \text{mean anomaly}$$

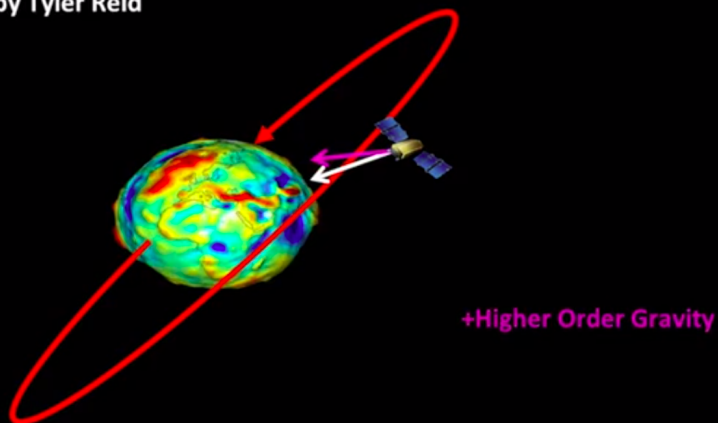
$$M = E - e \sin E \quad \text{Keplers equation}$$

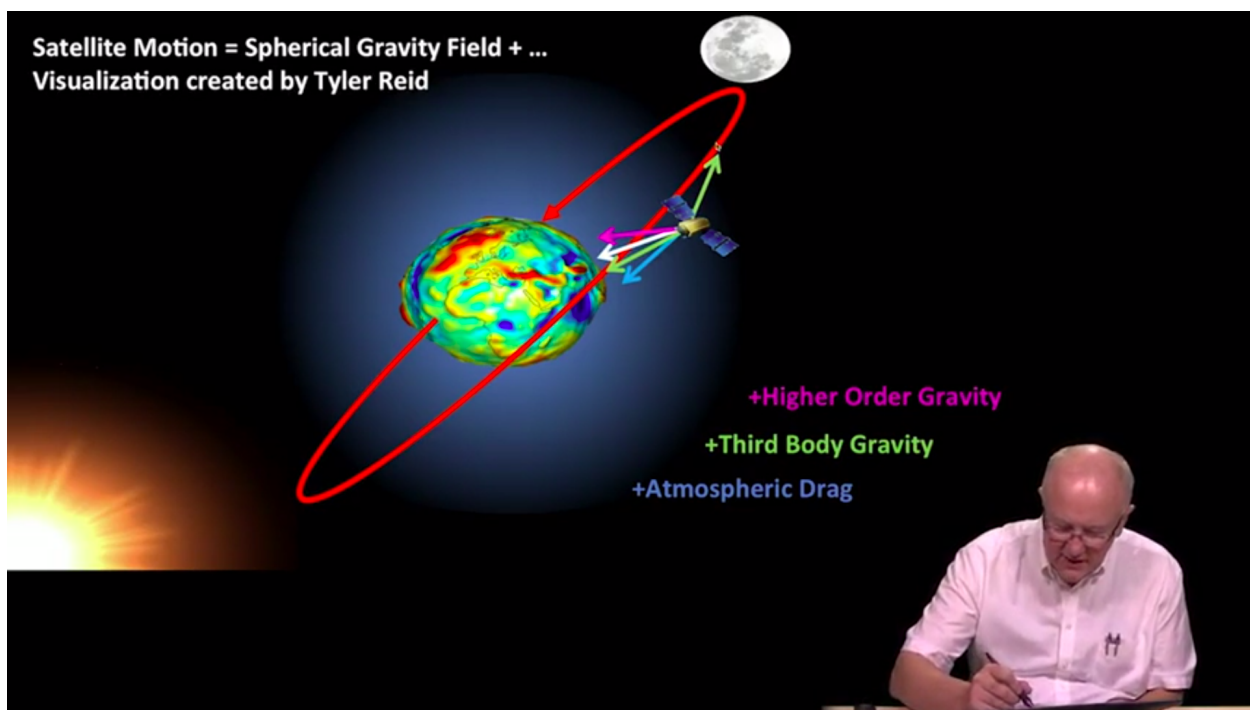
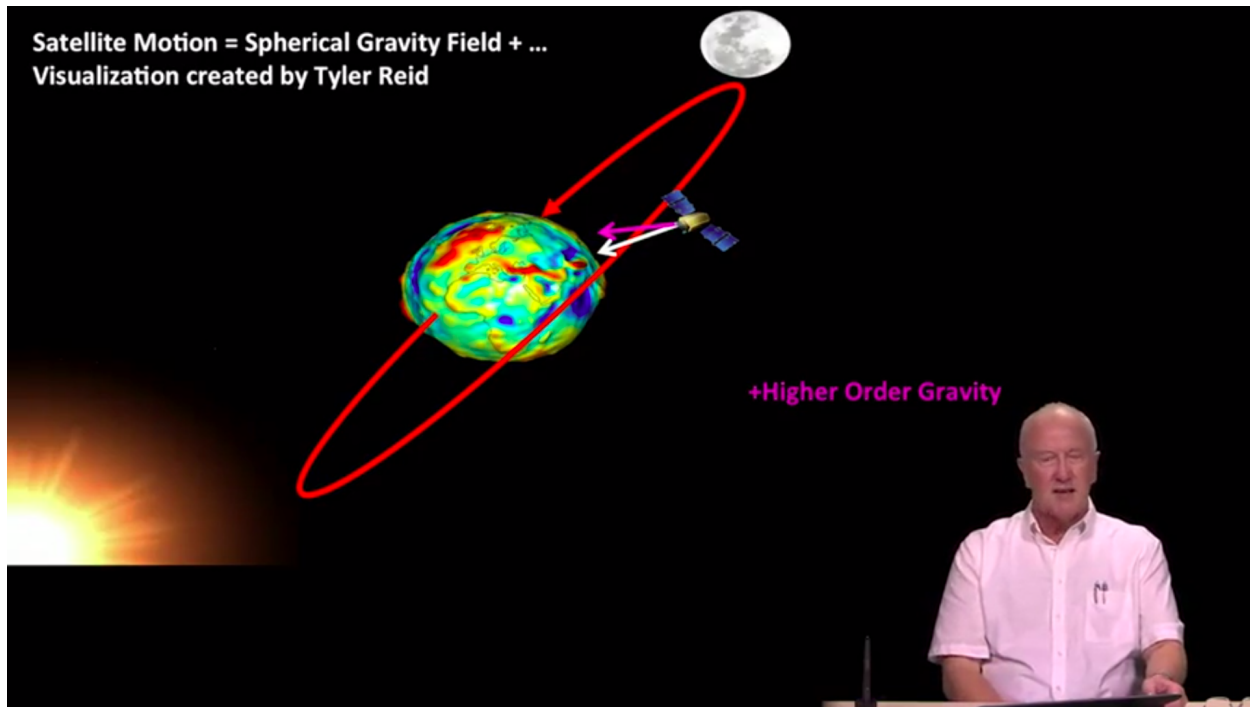
$$v = \tan^{-1} \left(\frac{\sqrt{1-e^2} \sin E}{\cos E - e} \right)$$



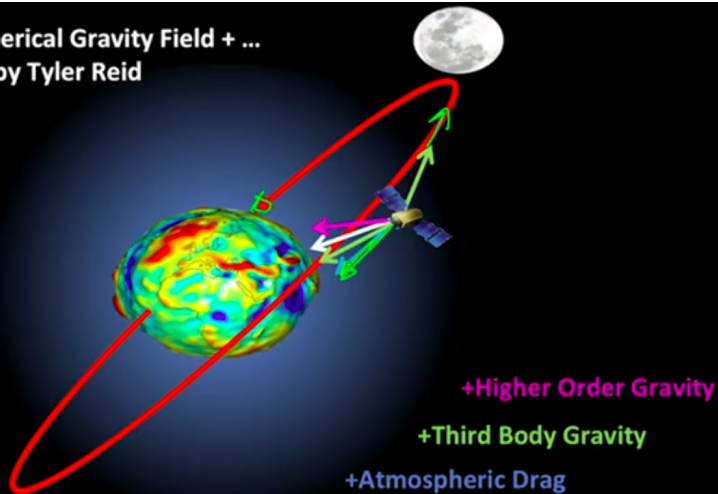
Satellite Motion = Spherical Gravity Field + ...

Visualization created by Tyler Reid

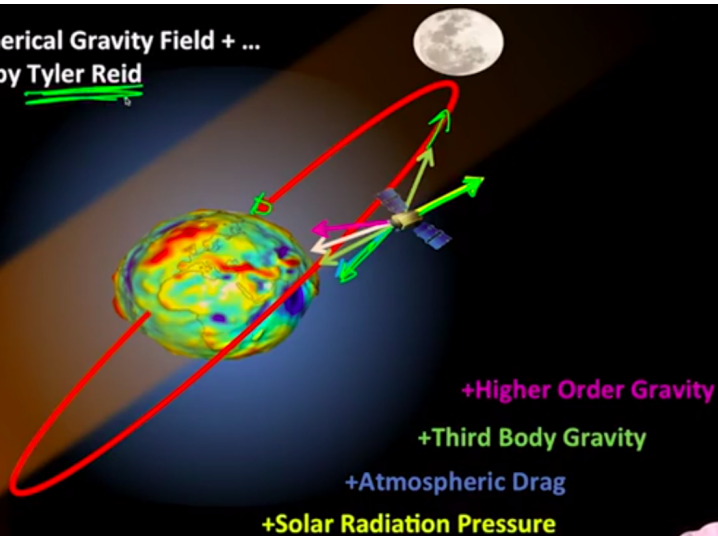




Satellite Motion = Spherical Gravity Field + ...
Visualization created by Tyler Reid



Satellite Motion = Spherical Gravity Field + ...
Visualization created by Tyler Reid



3.4 - Decoding the GPS navigation message

Parameter	Description
t_{0e}	ephemeris reference time
\sqrt{a}	square root of the semi-major axis
e	eccentricity
i_0	inclination angle at the reference time
Ω_0	longitude of the ascending node at the beginning of the GPS week
ω	argument of perigee
M_0	mean anomaly at the reference time
Δn	correction to the computed mean motion
\dot{i} (i -dot)	rate of change of inclination with time
$\dot{\Omega}$ (Ω -dot)	rate of change of RAAN with time
C_{uc}, C_{us}	amplitudes of harmonic correction terms for the computed argument of latitude
C_{rc}, C_{rs}	amplitudes of harmonic correction terms for the computed orbit radius
C_{ic}, C_{is}	amplitudes of harmonic correction terms for the computed inclination angle

◀ ▶ 🔍 11:57 / 14:24

Scroll for details



Table 4.3 Ephemeris parameters in the GPS navigation message

Parameter	Description
t_{0e}	ephemeris reference time
\sqrt{a}	square root of the semi-major axis
e	eccentricity
i_0	inclination angle at the reference time
Ω_0	longitude of the ascending node at the beginning of the GPS week
ω	argument of perigee
M_0	mean anomaly at the reference time
Δn	correction to the computed mean motion
\dot{i} (i -dot)	rate of change of inclination with time
$\dot{\Omega}$ (Ω -dot)	rate of change of RAAN with time
C_{uc}, C_{us}	amplitudes of harmonic correction terms for the computed argument of latitude
C_{rc}, C_{rs}	amplitudes of harmonic correction terms for the computed orbit radius
C_{ic}, C_{is}	amplitudes of harmonic correction terms for the computed inclination angle

◀ ▶ 🔍 11:57 / 14:24



Table 4.3 Ephemeris parameters in the GPS navigation message	
Parameter	Description
t_{0e}	ephemeris reference time
\sqrt{a}	square root of the semi-major axis
e	eccentricity
i_0	inclination angle at the reference time
Ω_0	longitude of the ascending node at the beginning of the GPS week
ω	argument of perigee
M_0	mean anomaly at the reference time
Δn	correction to the computed mean motion
\dot{i} (i -dot)	rate of change of inclination with time
$\dot{\Omega}$ (Ω -dot)	rate of change of RAAN with time
C_{uc}, C_{us}	amplitudes of harmonic correction terms for the computed argument of latitude
C_{rc}, C_{rs}	amplitudes of harmonic correction terms for the computed orbit radius
C_{ic}, C_{is}	amplitudes of harmonic correction terms for the computed inclination angle



Table 4.3 Ephemeris parameters in the GPS navigation message	
Parameter	Description
t_{0e}	ephemeris reference time
\sqrt{a}	square root of the semi-major axis
e	eccentricity
i_0	inclination angle at the reference time
Ω_0	longitude of the ascending node at the beginning of the GPS week
ω	argument of perigee
M_0	mean anomaly at the reference time
Δn	correction to the computed mean motion
\dot{i} (i -dot)	rate of change of inclination with time
$\dot{\Omega}$ (Ω -dot)	rate of change of RAAN with time
C_{uc}, C_{us}	amplitudes of harmonic correction terms for the computed argument of latitude
C_{rc}, C_{rs}	amplitudes of harmonic correction terms for the computed orbit radius
C_{ic}, C_{is}	amplitudes of harmonic correction terms for the computed inclination angle



Table 4.3 Ephemeris parameters in the GPS navigation message	
Parameter	Description
t_{0e}	ephemeris reference time
\sqrt{a}	square root of the semi-major axis
e	eccentricity
i_0	inclination angle at the reference time
Ω_0	longitude of the ascending node at the beginning of the GPS week
ω	argument of perigee
M_0	mean anomaly at the reference time
Δn	correction to the computed mean motion
\dot{i} (i -dot)	rate of change of inclination with time
$\dot{\Omega}$ (Ω -dot)	rate of change of RAAN with time
C_{uc}, C_{us}	amplitudes of harmonic correction terms for the computed argument of latitude
C_{rc}, C_{rs}	amplitudes of harmonic correction terms for the computed orbit radius
C_{ic}, C_{is}	amplitudes of harmonic correction terms for the computed inclination angle



Handwritten annotations on the table:

- A green circle highlights the first seven parameters: t_{0e} , \sqrt{a} , e , i_0 , Ω_0 , ω , and M_0 .
- A green circle highlights the last three parameters: C_{uc}, C_{us} , C_{rc}, C_{rs} , and C_{ic}, C_{is} .
- A green bracket labeled "secular" groups the parameters Δn , \dot{i} (i -dot), and $\dot{\Omega}$ (Ω -dot).
- A green bracket labeled "periodic" groups the parameters C_{uc}, C_{us} , C_{rc}, C_{rs} , and C_{ic}, C_{is} .

Table 4.3 Ephemeris parameters in the GPS navigation message	
Parameter	Description
t_{0e}	ephemeris reference time
\sqrt{a}	square root of the semi-major axis
e	eccentricity
i_0	inclination angle at the reference time
Ω_0	longitude of the ascending node at the beginning of the GPS week
ω	argument of perigee
M_0	mean anomaly at the reference time
Δn	correction to the computed mean motion
\dot{i} (i -dot)	rate of change of inclination with time
$\dot{\Omega}$ (Ω -dot)	rate of change of RAAN with time
C_{uc}, C_{us}	amplitudes of harmonic correction terms for the computed argument of latitude
C_{rc}, C_{rs}	amplitudes of harmonic correction terms for the computed orbit radius
C_{ic}, C_{is}	amplitudes of harmonic correction terms for the computed inclination angle



Handwritten annotations on the table:

- A green circle highlights the first seven parameters: t_{0e} , \sqrt{a} , e , i_0 , Ω_0 , ω , and M_0 .
- A green circle highlights the last three parameters: C_{uc}, C_{us} , C_{rc}, C_{rs} , and C_{ic}, C_{is} .
- A green bracket labeled "secular" groups the parameters Δn , \dot{i} (i -dot), and $\dot{\Omega}$ (Ω -dot).
- A green bracket labeled "periodic" groups the parameters C_{uc}, C_{us} , C_{rc}, C_{rs} , and C_{ic}, C_{is} .

Module 3: Orbits & Signals

GNSS Orbits

- 3.1 Brahe, Kepler & Newton
- 3.2 Coordinate frames
- 3.3 Transforming from Keplerian parameters to ECEF
- 3.4 Decoding the GPS navigation message

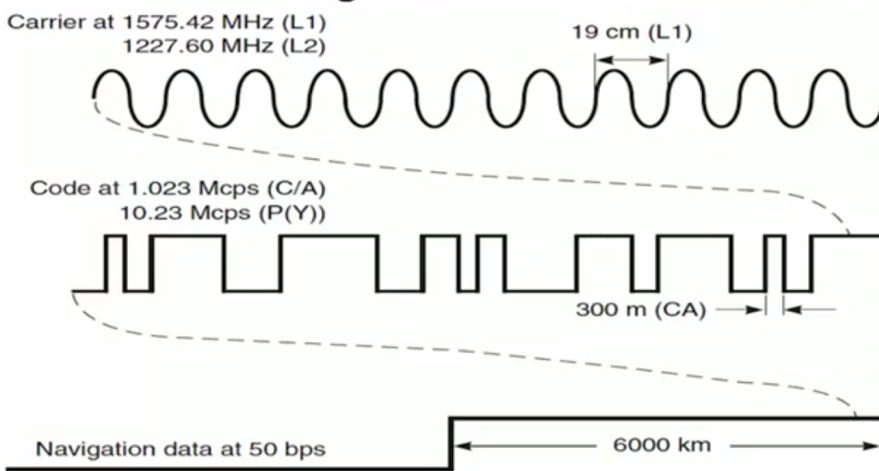
GNSS Signals

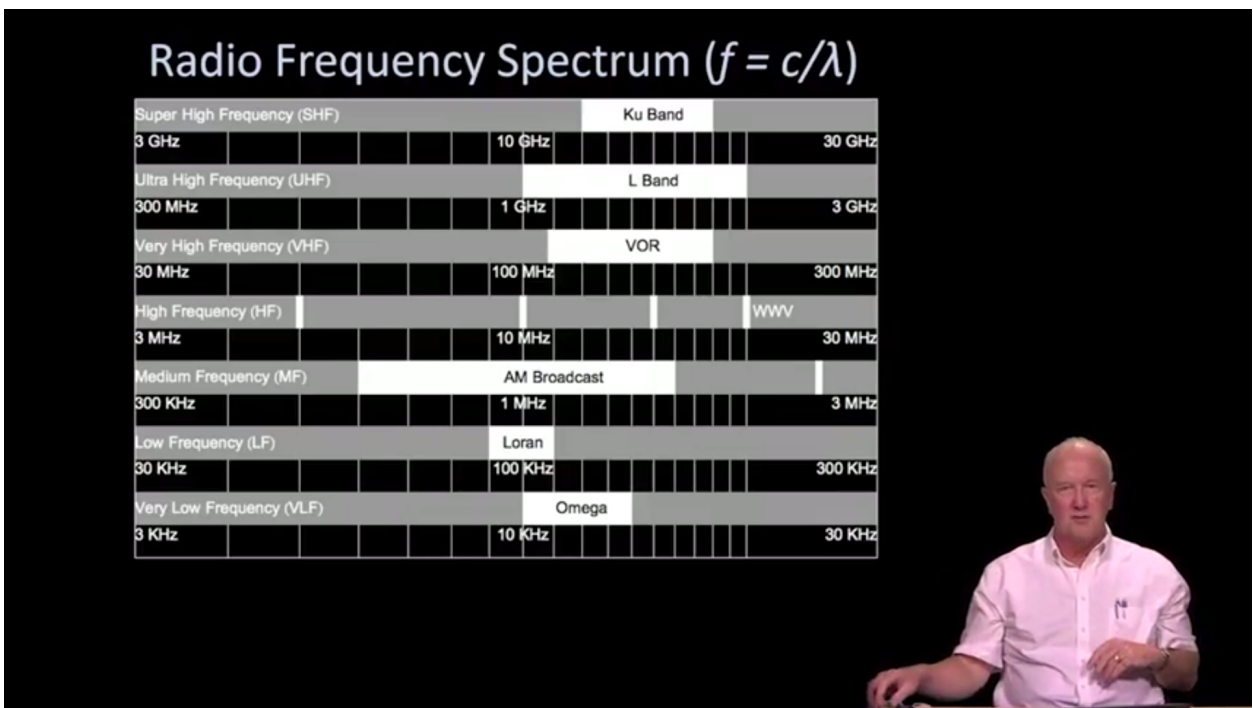
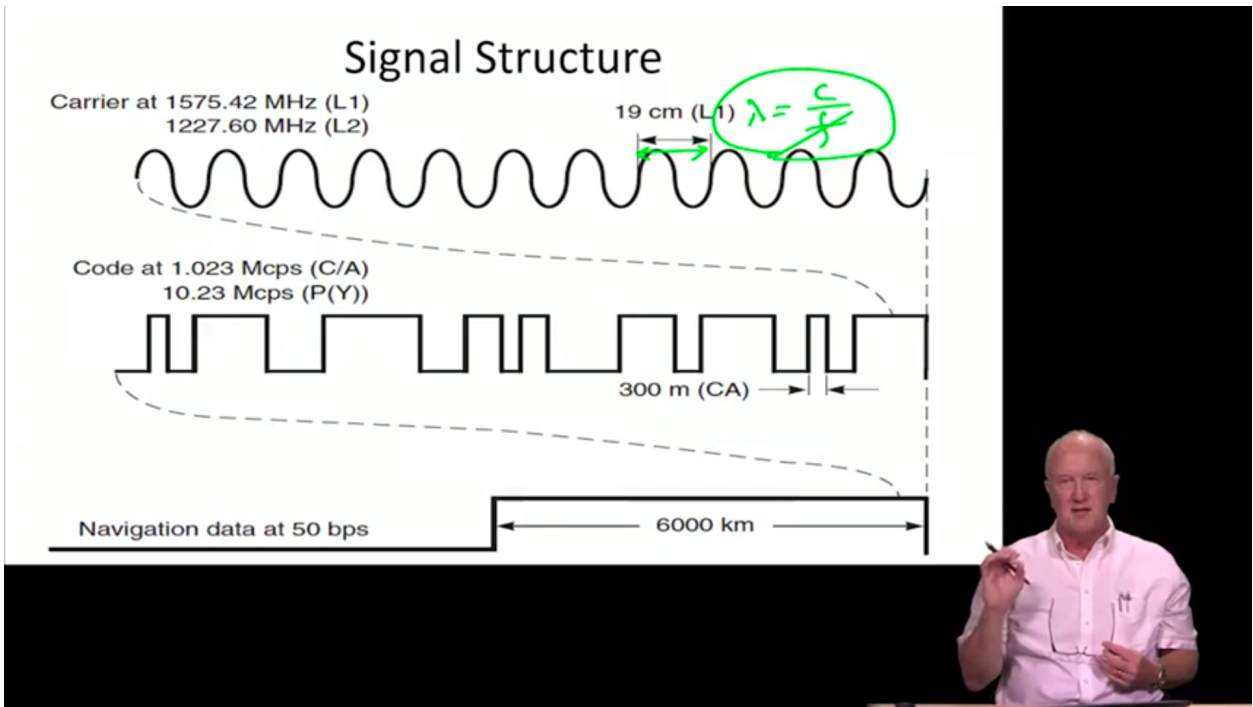
3.5 L band

- 3.6 Frequency domain
- 3.7 Amplitude spectra of GNSS signals
- 3.8 Auto-correlation & Cross-correlation
- 3.9 New GNSS signals

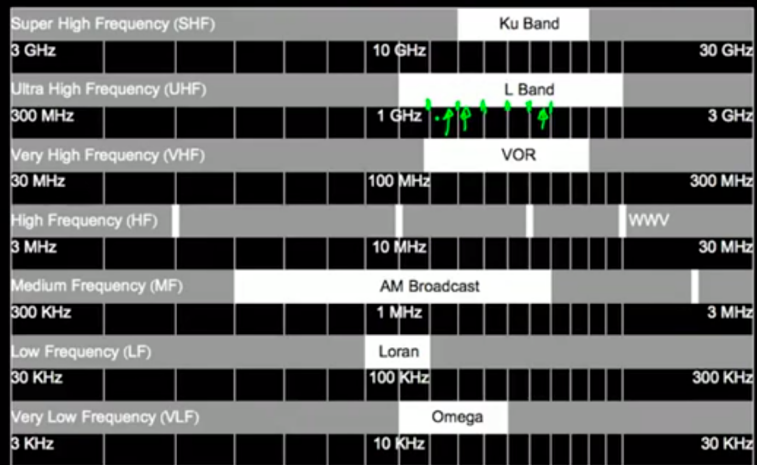


Signal Structure

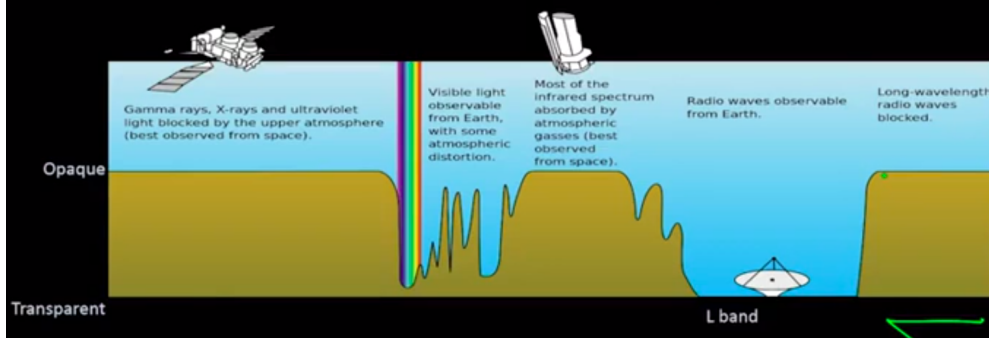




Radio Frequency Spectrum ($f = c/\lambda$)



Atmospheric Opacity



http://upload.wikimedia.org/wikipedia/commons/3/34/Atmospheric_electromagnetic_opacity.svg

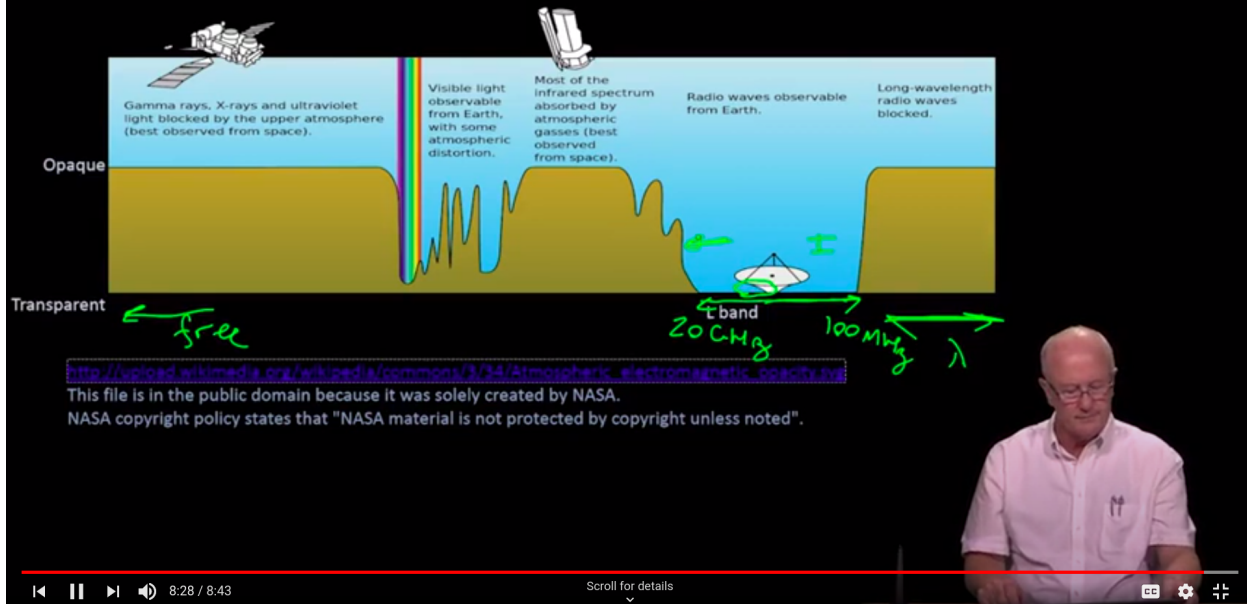
This file is in the public domain because it was solely created by NASA.

NASA copyright policy states that "NASA material is not protected by copyright unless noted".



≡ 3.5 - Fourier series, Pulses, Amplitude spectra of GPS signals

Atmospheric Opacity



Module 3: Orbits & Signals

GNSS Orbits

- 3.1 Brahe, Kepler & Newton
- 3.2 Coordinate frames
- 3.3 Transforming from Keplerian parameters to ECEF
- 3.4 Decoding the GPS navigation message

GNSS Signals

- 3.5 L band
- 3.6 Frequency domain**
- 3.7 Amplitude spectra of GNSS signals
- 3.8 Auto-correlation & Cross-correlation
- 3.9 New GNSS signals

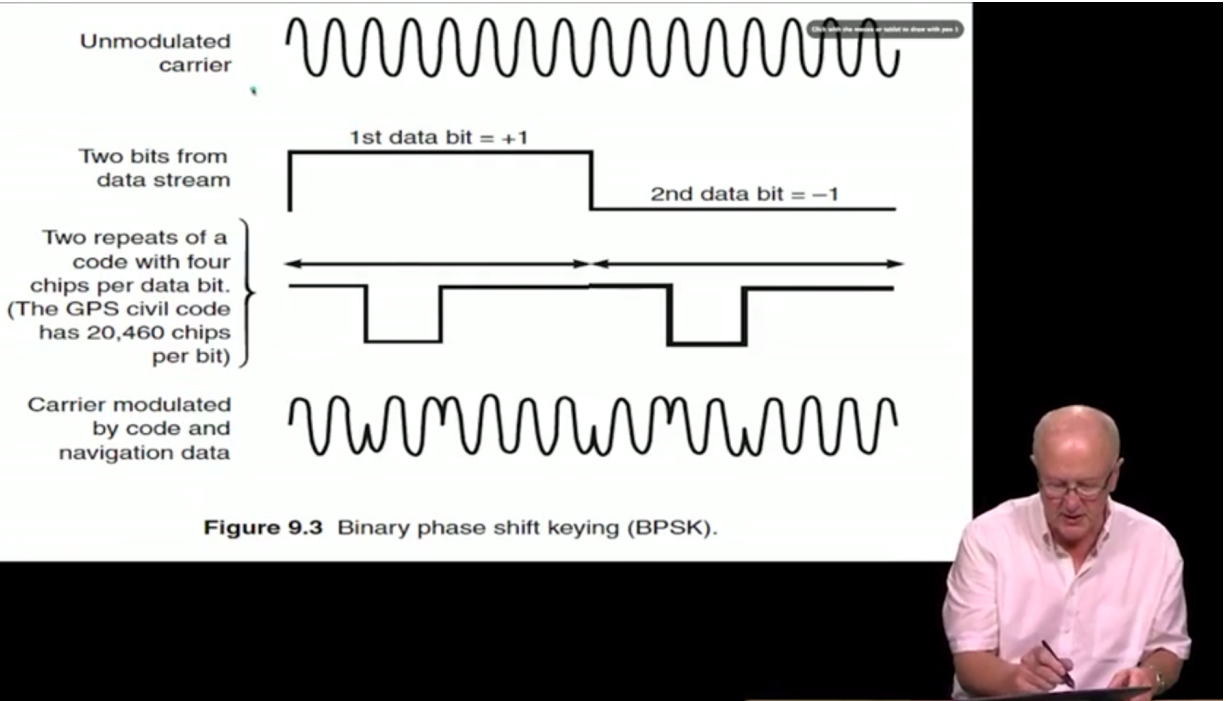


Figure 9.3 Binary phase shift keying (BPSK).

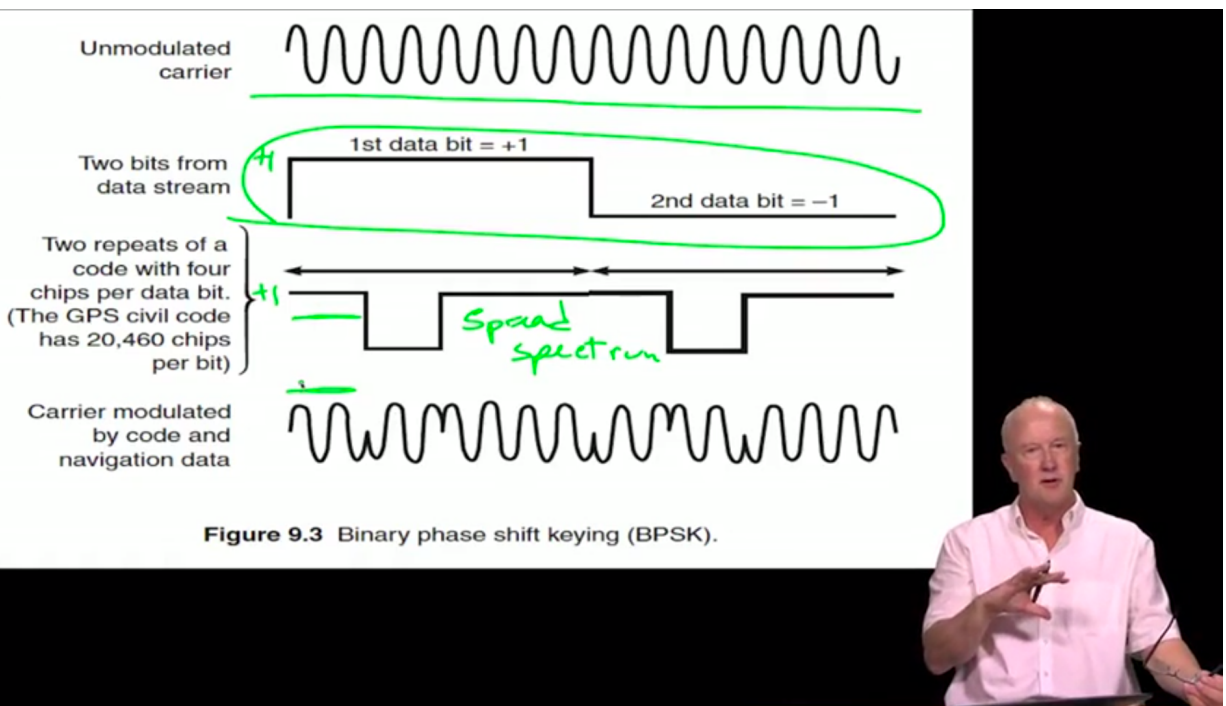
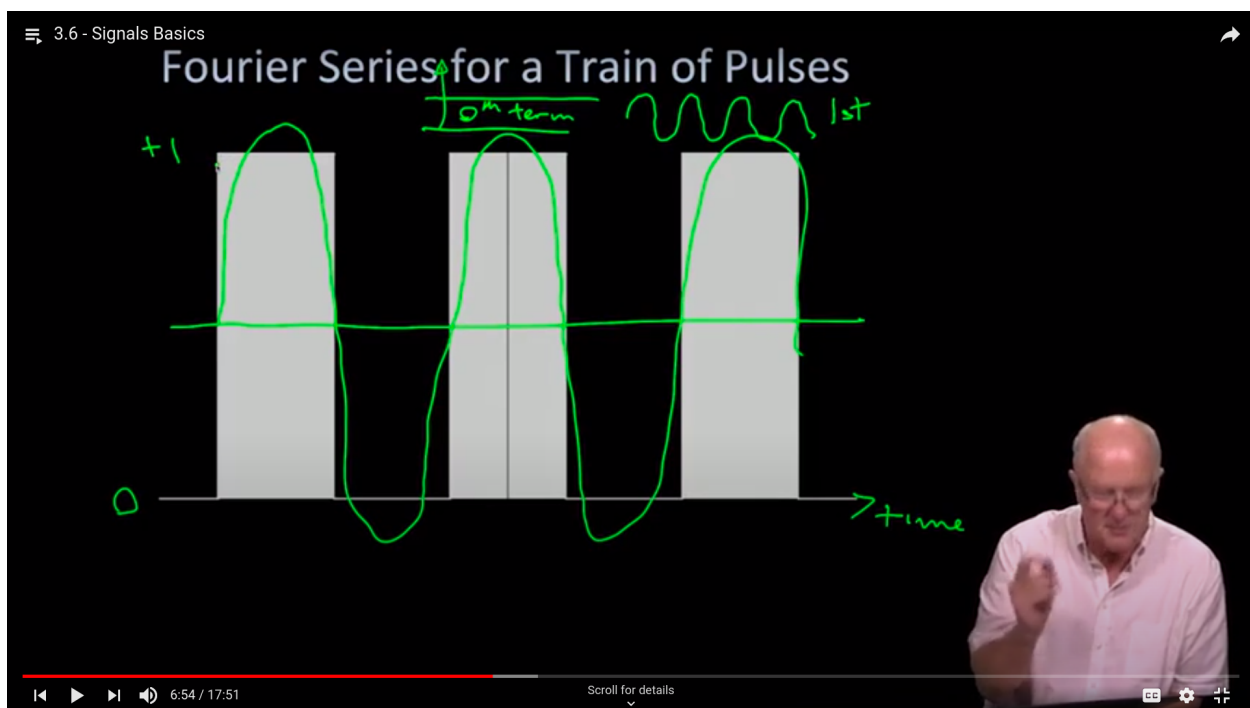
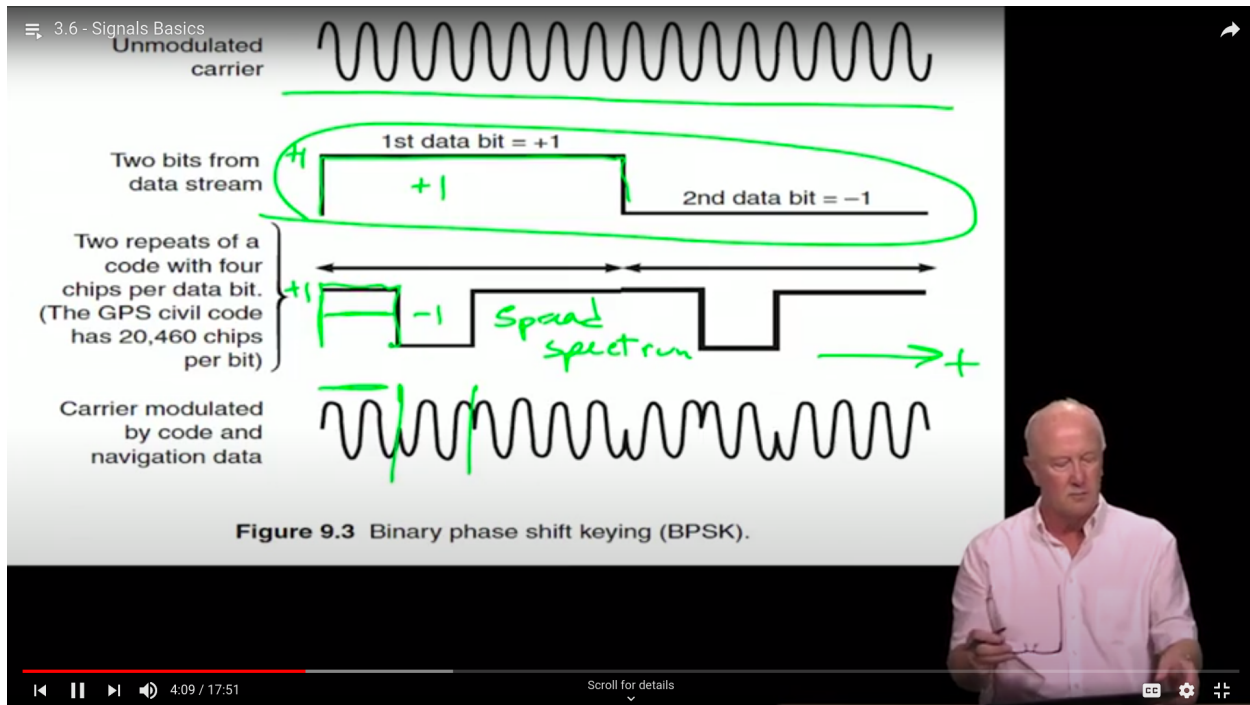
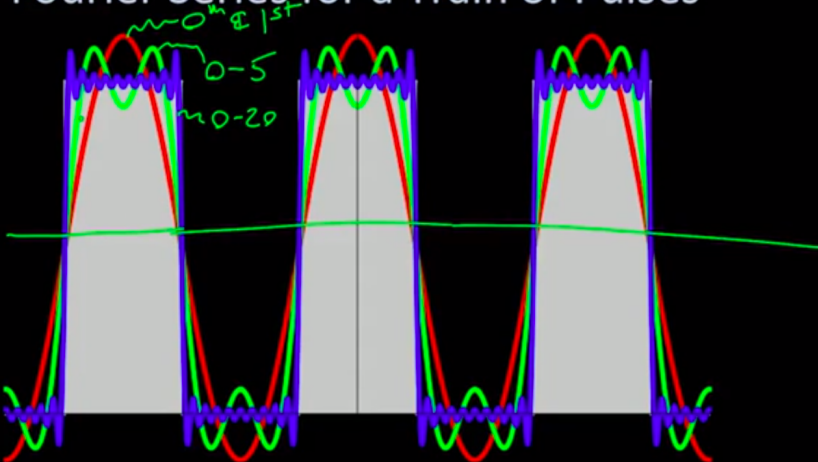


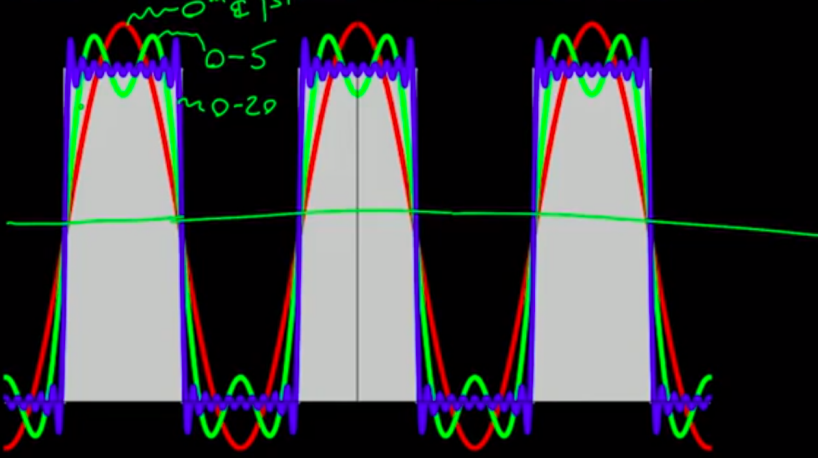
Figure 9.3 Binary phase shift keying (BPSK).



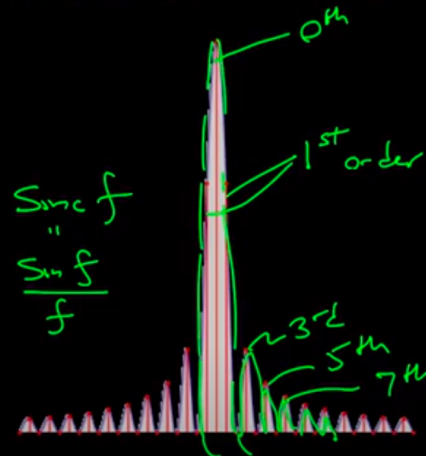
Fourier Series for a Train of Pulses



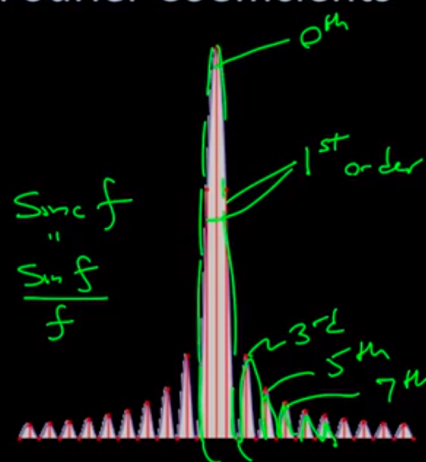
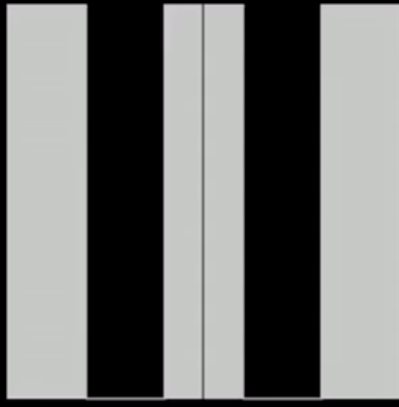
Fourier Series for a Train of Pulses



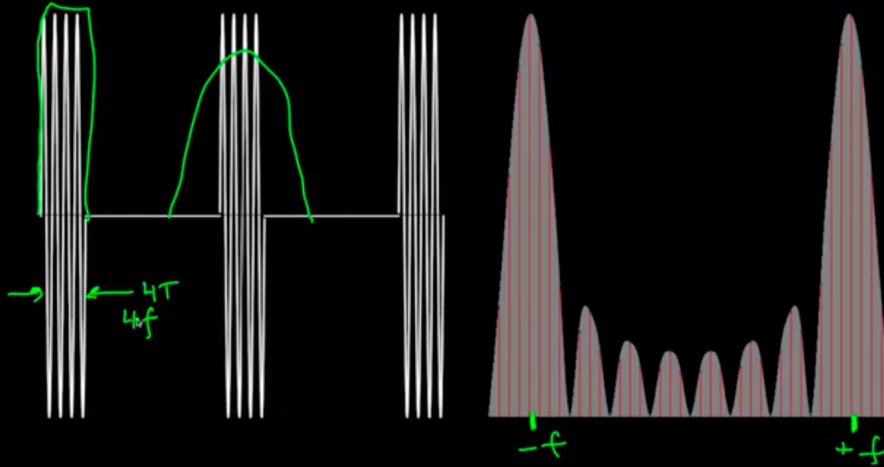
Baseband Pulses & Fourier Coefficients



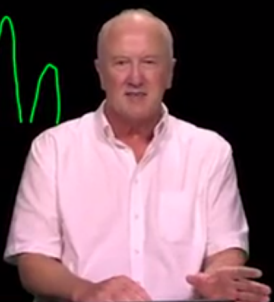
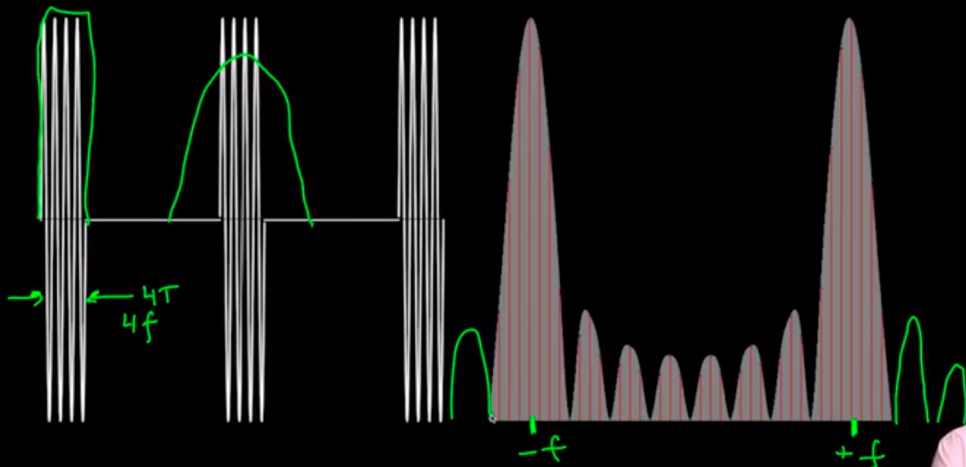
Baseband Pulses & Fourier Coefficients



RF Pulses & Fourier Coefficients



RF Pulses & Fourier Coefficients



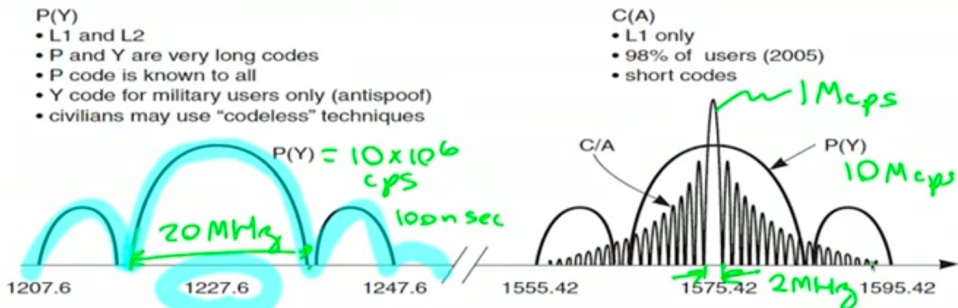


Figure 9.4 Amplitude spectrum of GPS signal in mid-2005 with $f_{L1} = 1575.42$ MHz and $f_{L2} = 1227.60$ MHz. Only positive frequencies are shown.

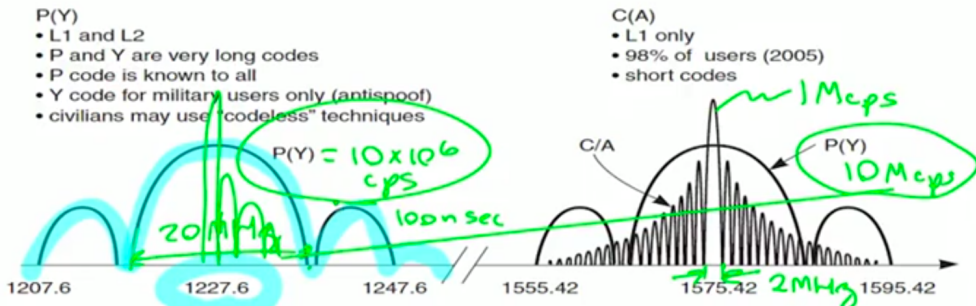


Figure 9.4 Amplitude spectrum of GPS signal in mid-2005 with $f_{L1} = 1575.42$ MHz and $f_{L2} = 1227.60$ MHz. Only positive frequencies are shown.



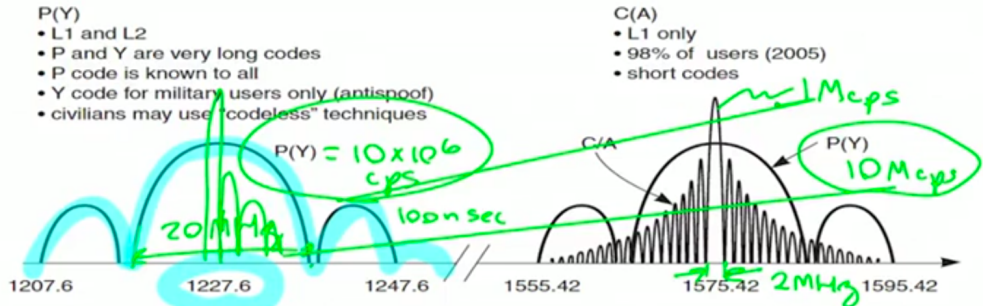
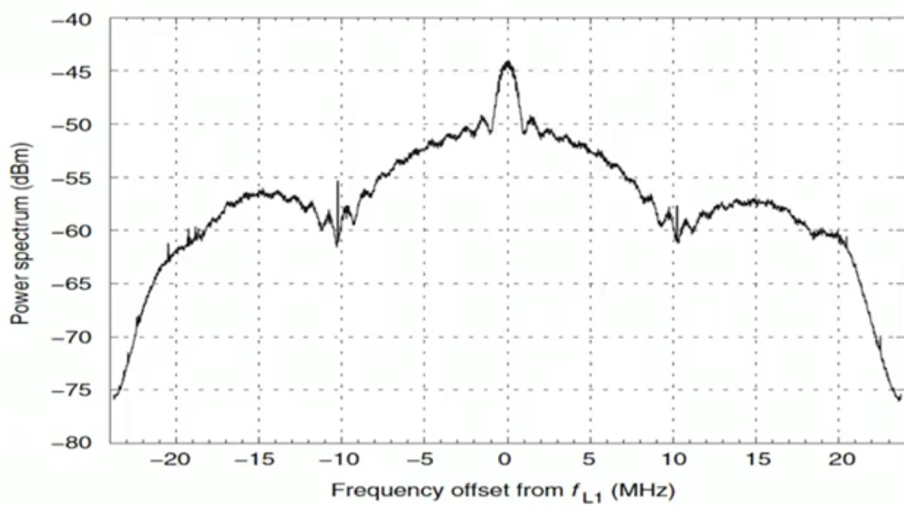
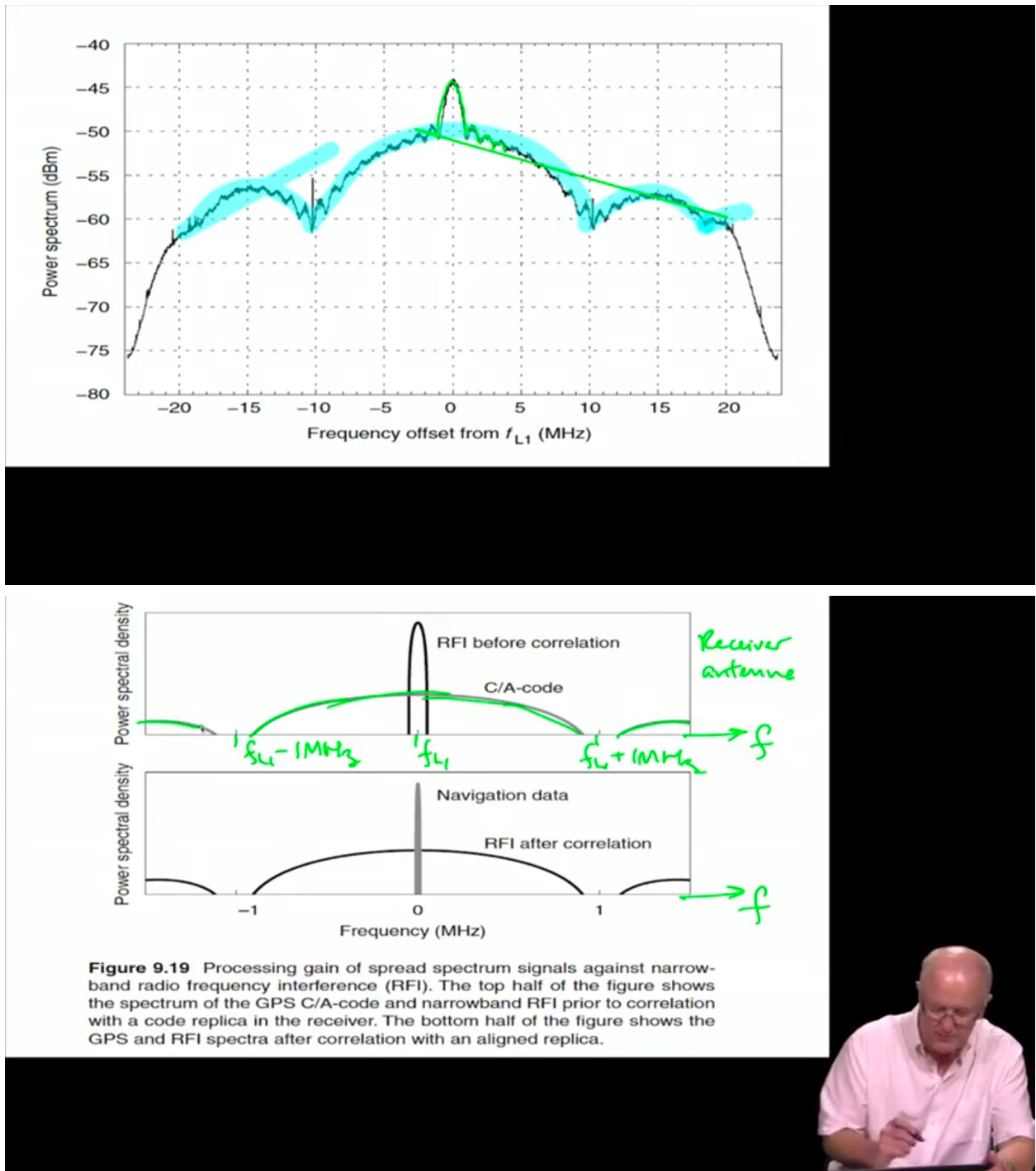


Figure 9.4 Amplitude spectrum of GPS signal in mid-2005 with $f_{L1} = 1575.42$ MHz and $f_{L2} = 1227.60$ MHz. Only positive frequencies are shown.





3.7 - Amplitude Spectra

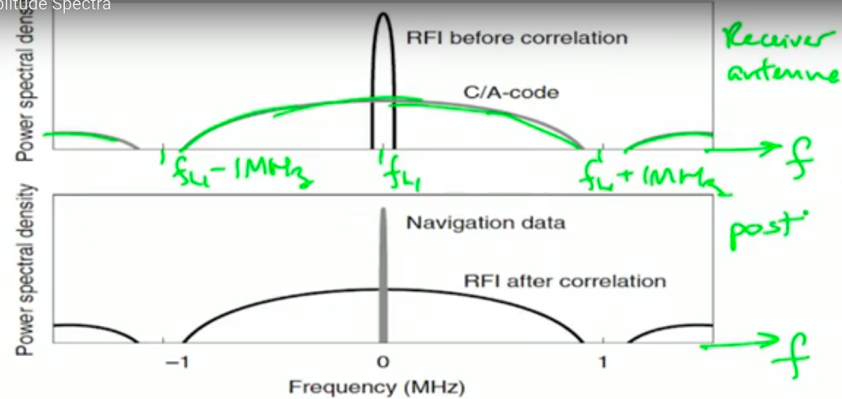


Figure 9.19 Processing gain of spread spectrum signals against narrowband radio frequency interference (RFI). The top half of the figure shows the spectrum of the GPS C/A-code and narrowband RFI prior to correlation with a code replica in the receiver. The bottom half of the figure shows the GPS and RFI spectra after correlation with an aligned replica.

◀ ▶ 🔍 7:35 / 12:32

Scroll for details

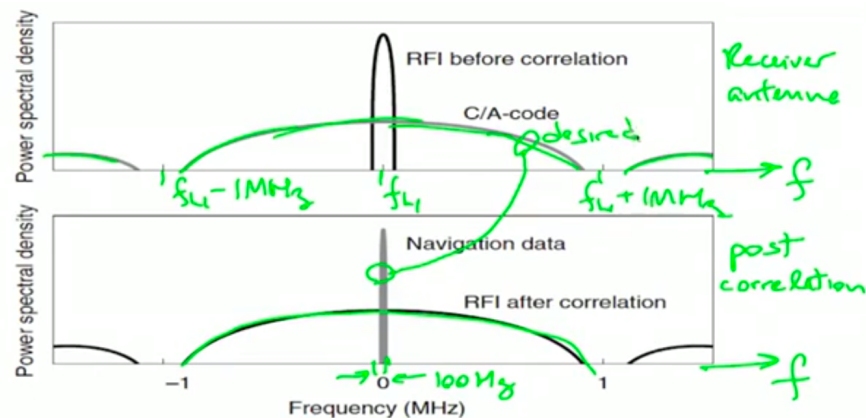
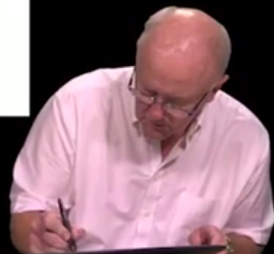


Figure 9.19 Processing gain of spread spectrum signals against narrowband radio frequency interference (RFI). The top half of the figure shows the spectrum of the GPS C/A-code and narrowband RFI prior to correlation with a code replica in the receiver. The bottom half of the figure shows the GPS and RFI spectra after correlation with an aligned replica.



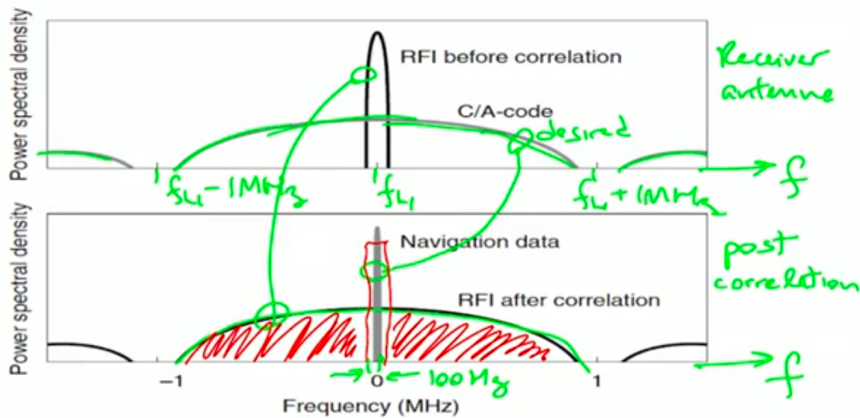


Figure 9.19 Processing gain of spread spectrum signals against narrowband radio frequency interference (RFI). The top half of the figure shows the spectrum of the GPS C/A-code and narrowband RFI prior to correlation with a code replica in the receiver. The bottom half of the figure shows the GPS and RFI spectra after correlation with an aligned replica.

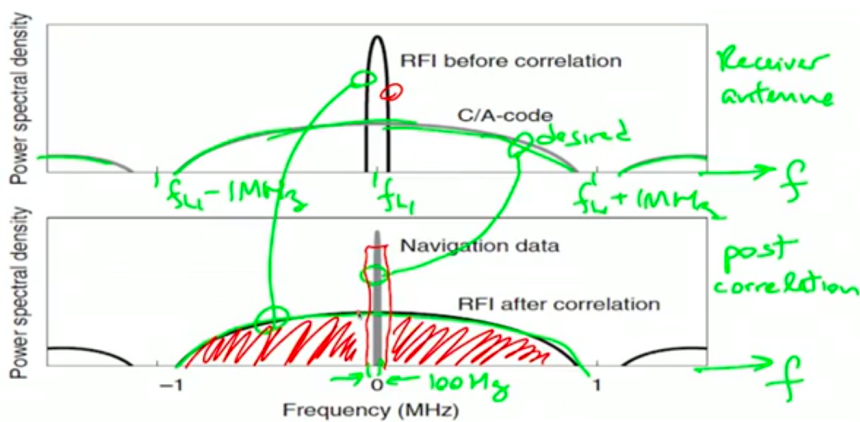
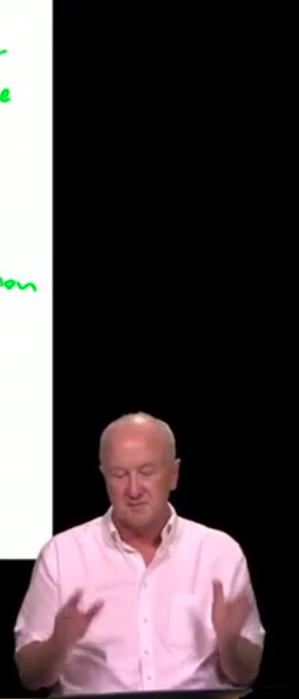
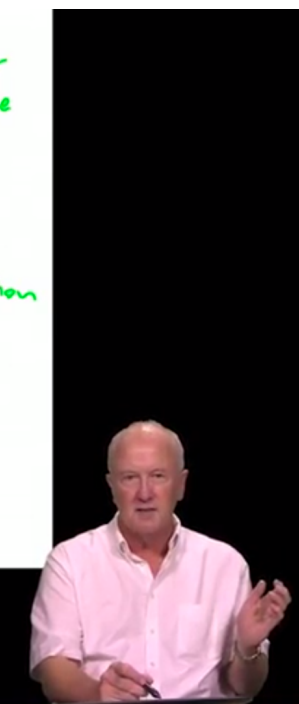


Figure 9.19 Processing gain of spread spectrum signals against narrowband radio frequency interference (RFI). The top half of the figure shows the spectrum of the GPS C/A-code and narrowband RFI prior to correlation with a code replica in the receiver. The bottom half of the figure shows the GPS and RFI spectra after correlation with an aligned replica.



3.7 - Amplitude Spectra

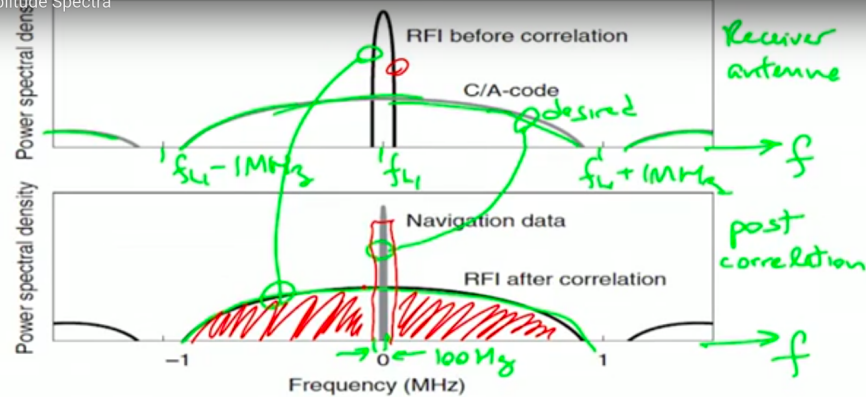


Figure 9.19 Processing gain of spread spectrum signals against narrowband radio frequency interference (RFI). The top half of the figure shows the spectrum of the GPS C/A-code and narrowband RFI prior to correlation with a code replica in the receiver. The bottom half of the figure shows the GPS and RFI spectra after correlation with an aligned replica.

◀ ▶ 🔍 12:13 / 12:32

Scroll for details

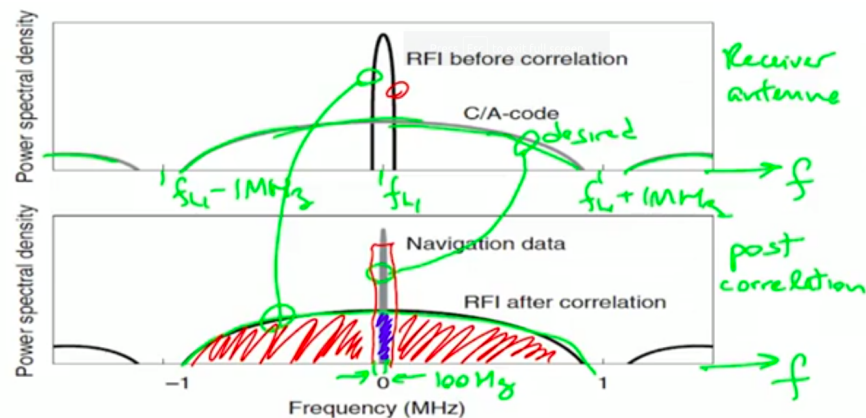
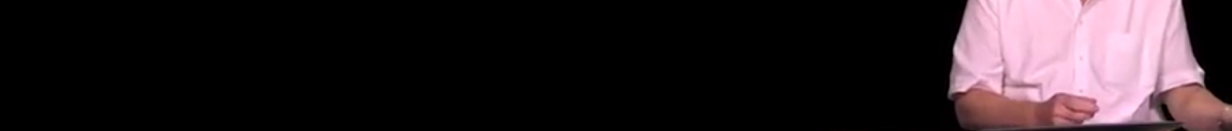


Figure 9.19 Processing gain of spread spectrum signals against narrowband radio frequency interference (RFI). The top half of the figure shows the spectrum of the GPS C/A-code and narrowband RFI prior to correlation with a code replica in the receiver. The bottom half of the figure shows the GPS and RFI spectra after correlation with an aligned replica.



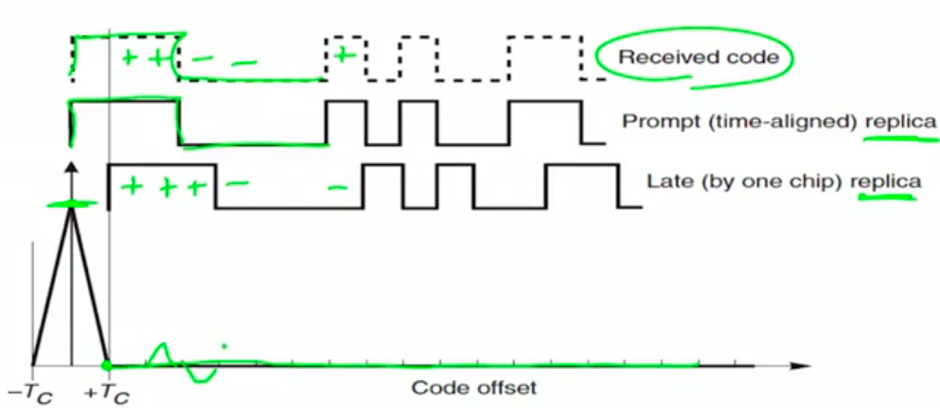


Figure 9.6 Correlation of the received code with time-shifted replicas. The correlation function that is shown is close to the ideal for ranging signals. It has a peak that is sharp and unique.

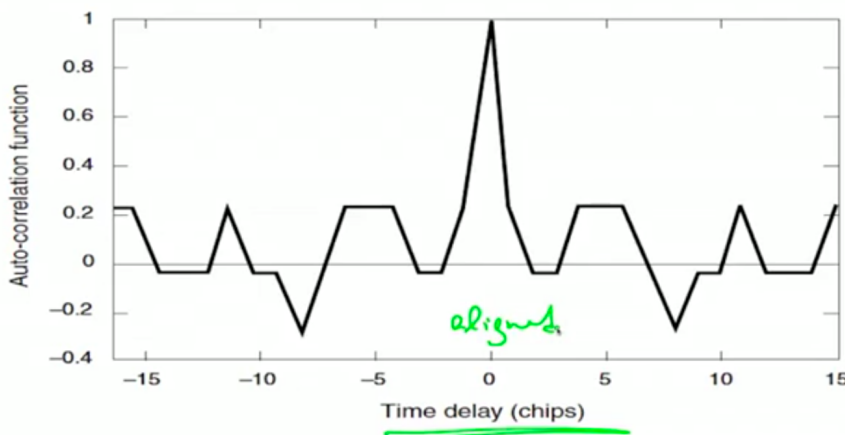
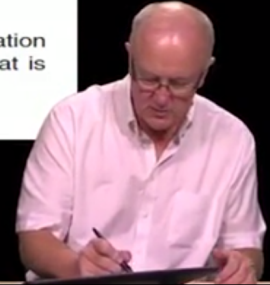


Figure 9.13 Auto-correlation function for an $N = 31$ Gold sequence. Like the auto-correlation function for all Gold codes, this function takes only four values. For this length-31 code, those values are $\{1, -1/31, -9/31, 7/31\}$.



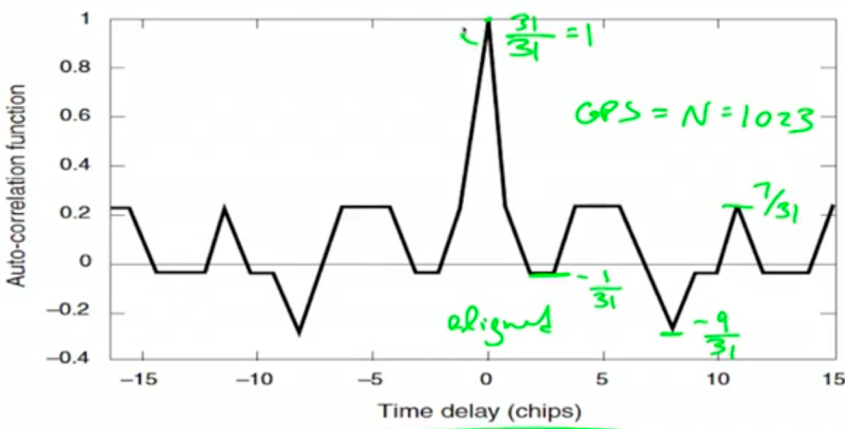


Figure 9.13 Auto-correlation function for an $N = 31$ Gold sequence. Like the auto-correlation function for all Gold codes, this function takes only four values. For this length-31 code, those values are $\{1, -1/31, -9/31, 7/31\}$.



3.8 - Auto correlation and cross correlation

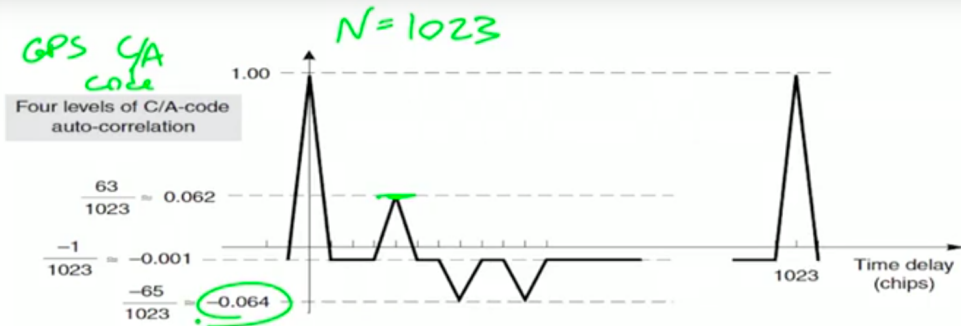
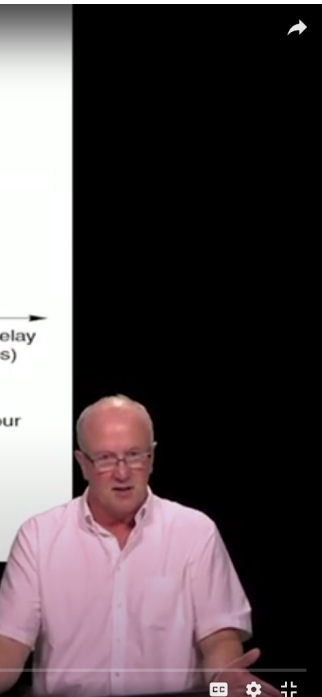


Figure 9.14 Auto-correlation for the C/A-codes. This auto-correlation function takes only the four values that are shown above, but there are many more sidelobes than shown.



3.8 - Auto correlation and cross correlation

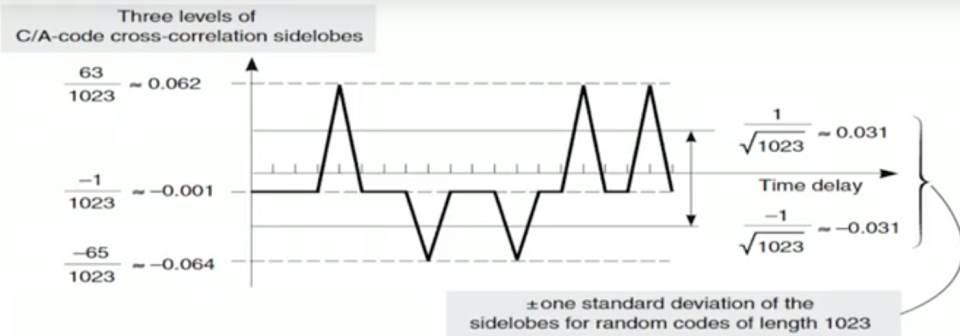


Figure 9.15 Cross-correlation function for the C/A-codes. These functions take only the three values shown above, but there are many more sidelobes than shown. As shown, random codes predict the sidelobe values with fair accuracy.

3.8 - Auto correlation and cross correlation

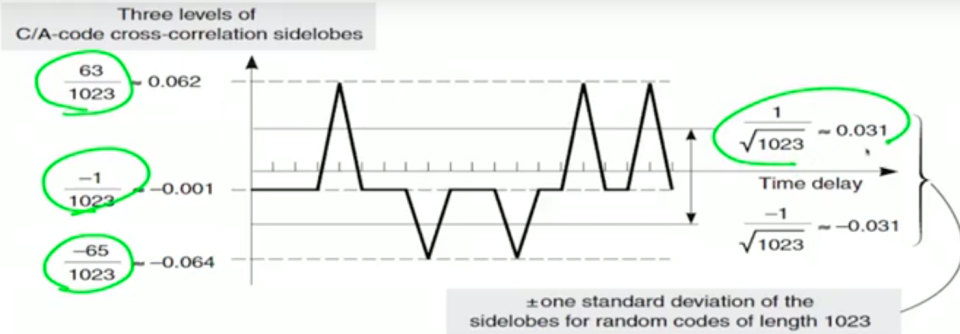


Figure 9.15 Cross-correlation function for the C/A-codes. These functions take only the three values shown above, but there are many more sidelobes than shown. As shown, random codes predict the sidelobe values with fair accuracy.

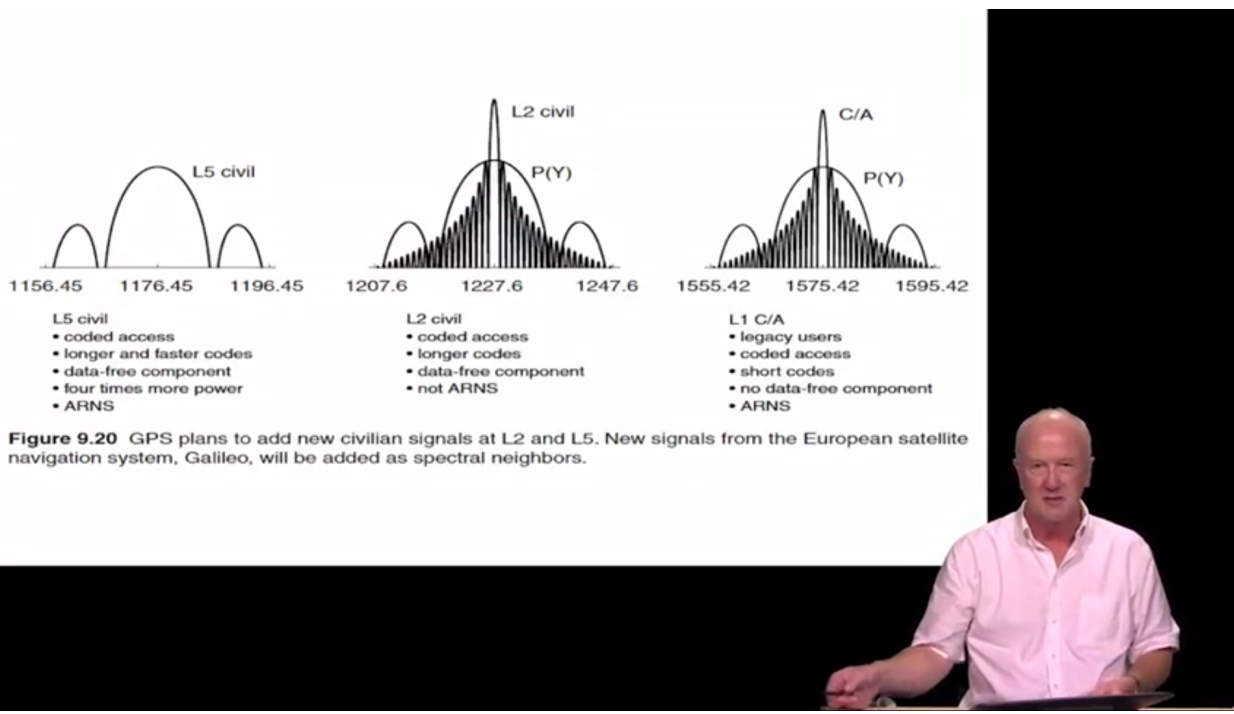


Figure 9.20 GPS plans to add new civilian signals at L2 and L5. New signals from the European satellite navigation system, Galileo, will be added as spectral neighbors.

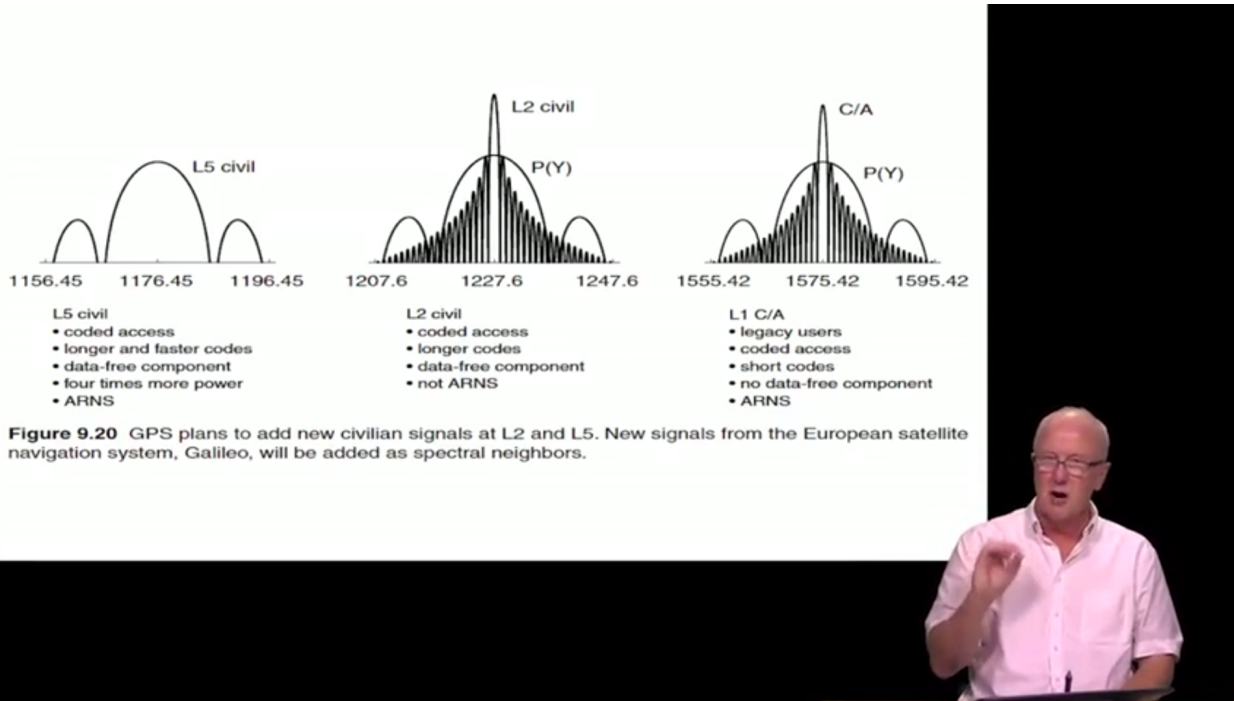


Figure 9.20 GPS plans to add new civilian signals at L2 and L5. New signals from the European satellite navigation system, Galileo, will be added as spectral neighbors.

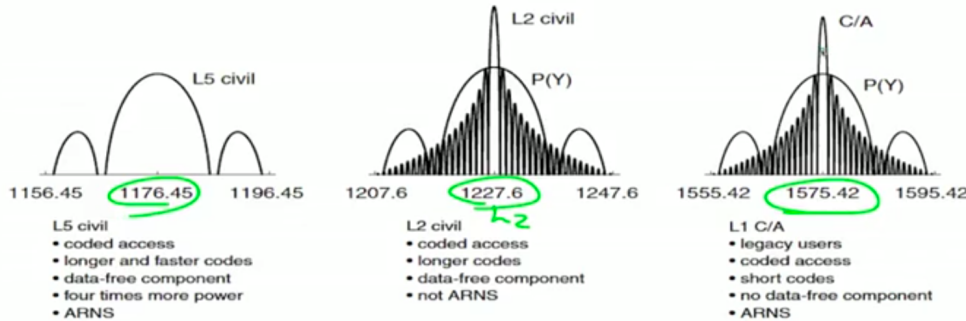


Figure 9.20 GPS plans to add new civilian signals at L2 and L5. New signals from the European satellite navigation system, Galileo, will be added as spectral neighbors.

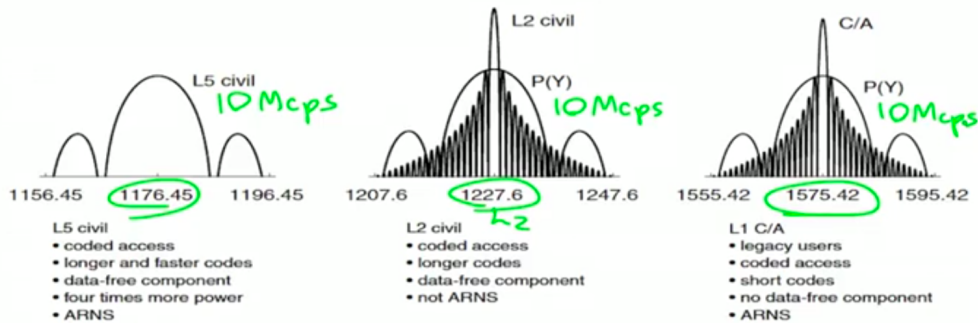
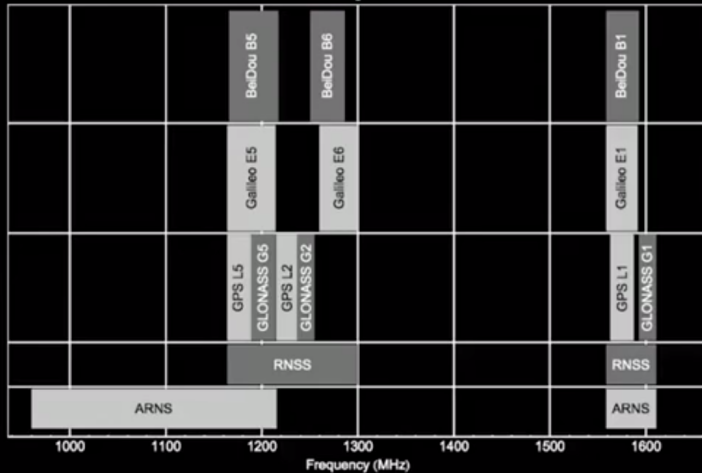


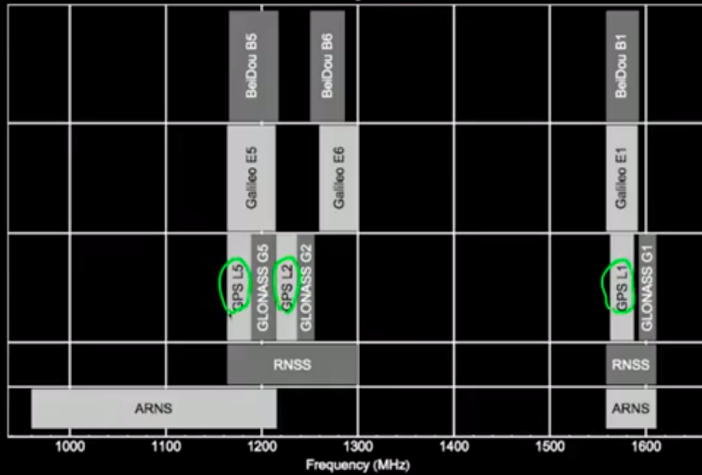
Figure 9.20 GPS plans to add new civilian signals at L2 and L5. New signals from the European satellite navigation system, Galileo, will be added as spectral neighbors.

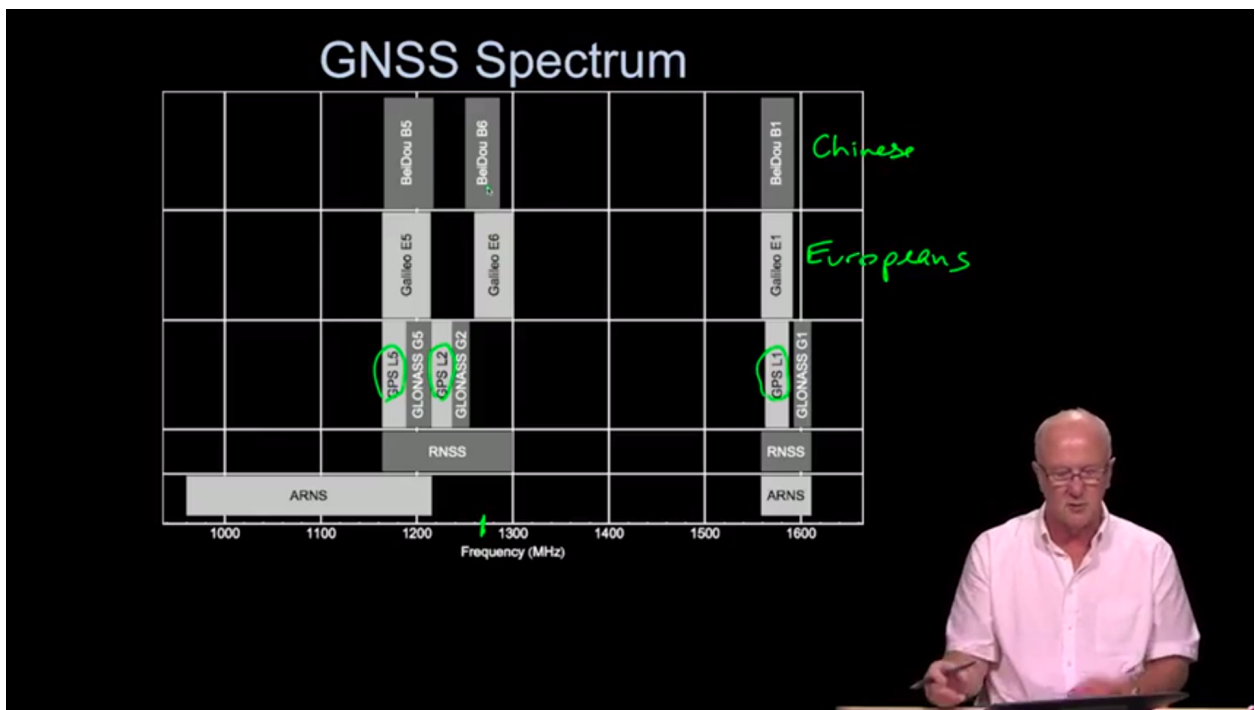
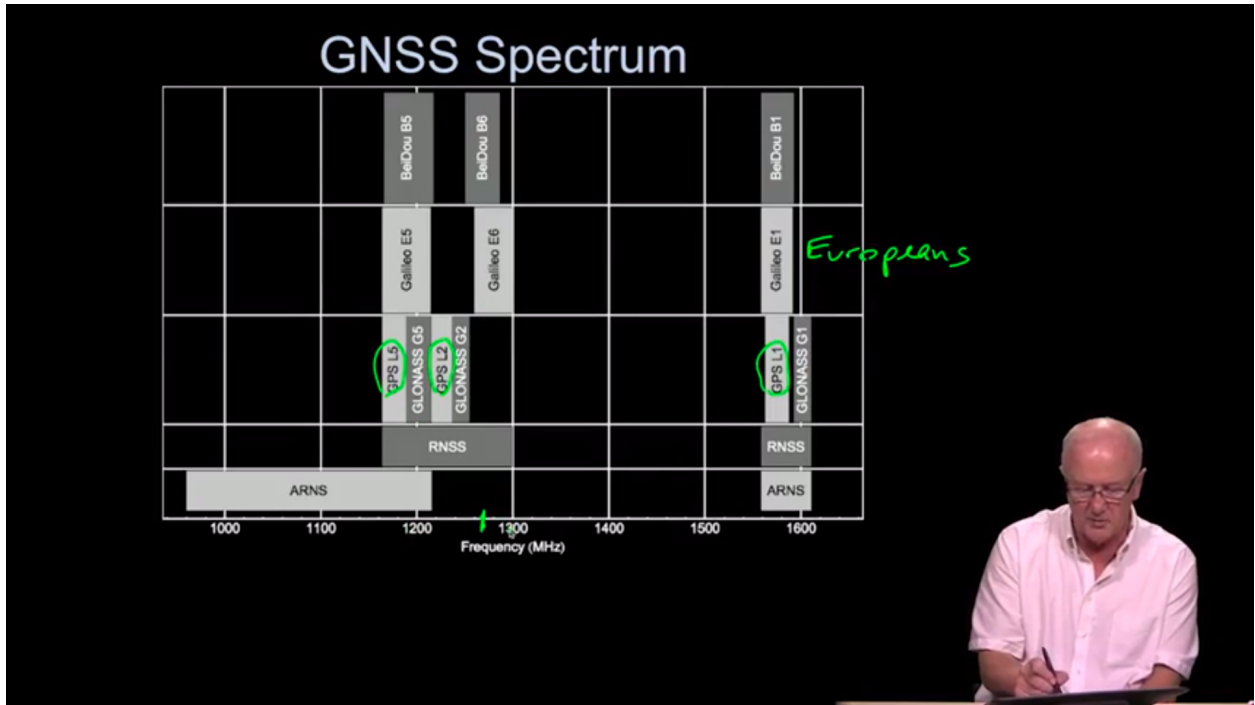


GNSS Spectrum



GNSS Spectrum





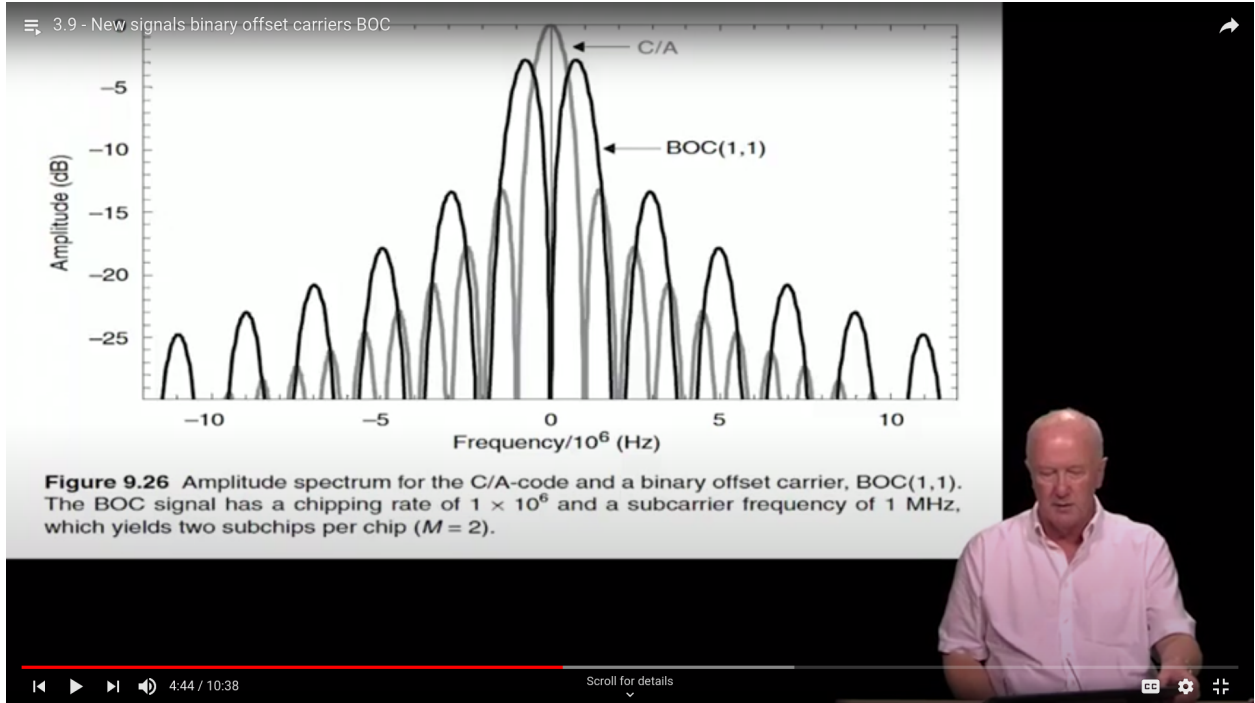
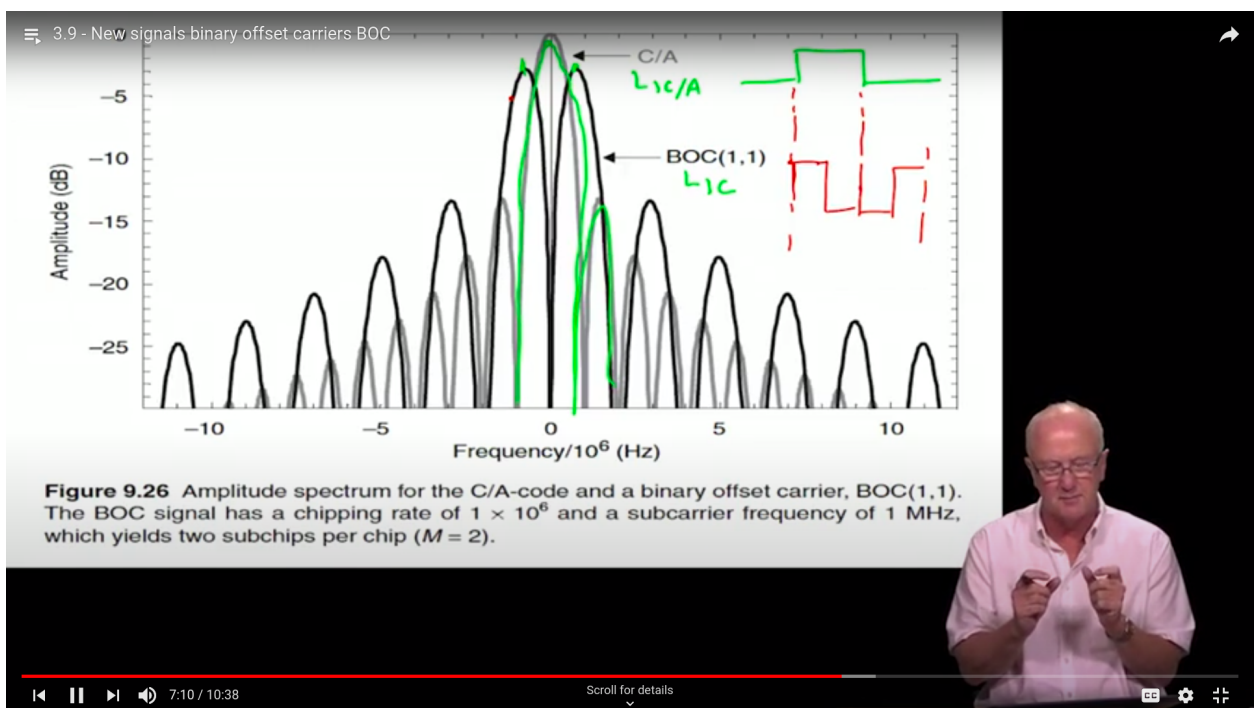


Figure 9.26 Amplitude spectrum for the C/A-code and a binary offset carrier, BOC(1,1). The BOC signal has a chipping rate of 1×10^6 and a subcarrier frequency of 1 MHz, which yields two subchips per chip ($M = 2$).



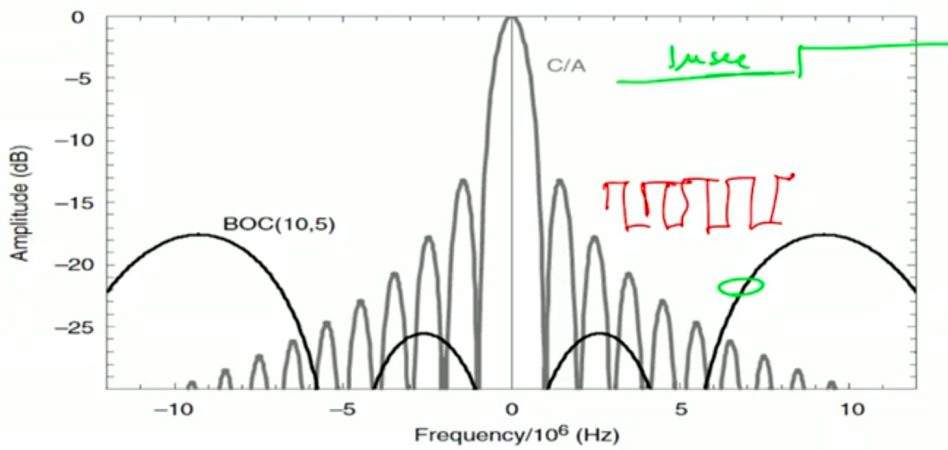
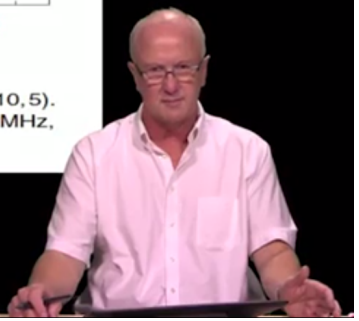
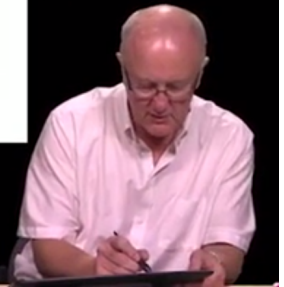
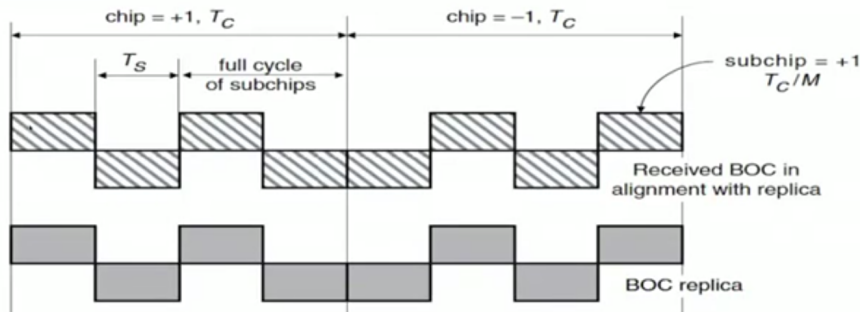


Figure 9.27 Amplitude spectrum for the C/A-code and a binary offset carrier, BOC(10,5). The BOC signal has a chipping rate of 5×10^6 and a subcarrier frequency of 10 MHz, which yields four subchips per chip ($M = 4$).



Binary Offset Carriers



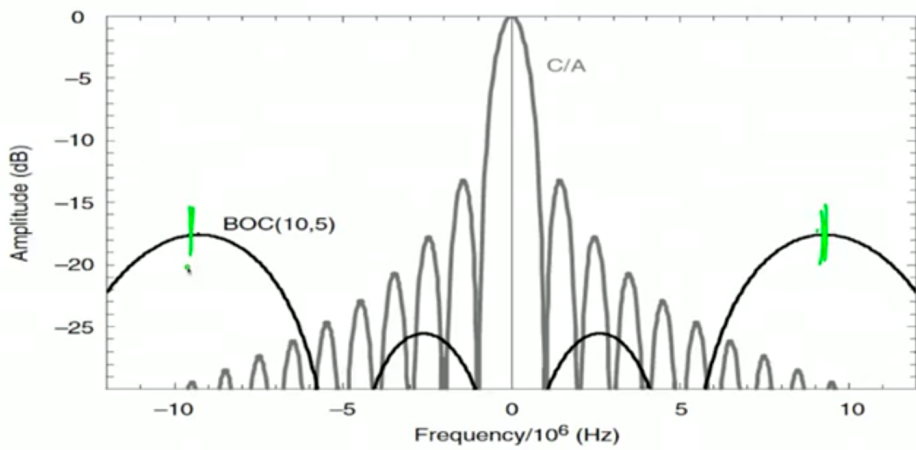


Figure 9.27 Amplitude spectrum for the C/A-code and a binary offset carrier, BOC(10,5). The BOC signal has a chipping rate of 5×10^6 and a subcarrier frequency of 10 MHz, which yields four subchips per chip ($M = 4$).

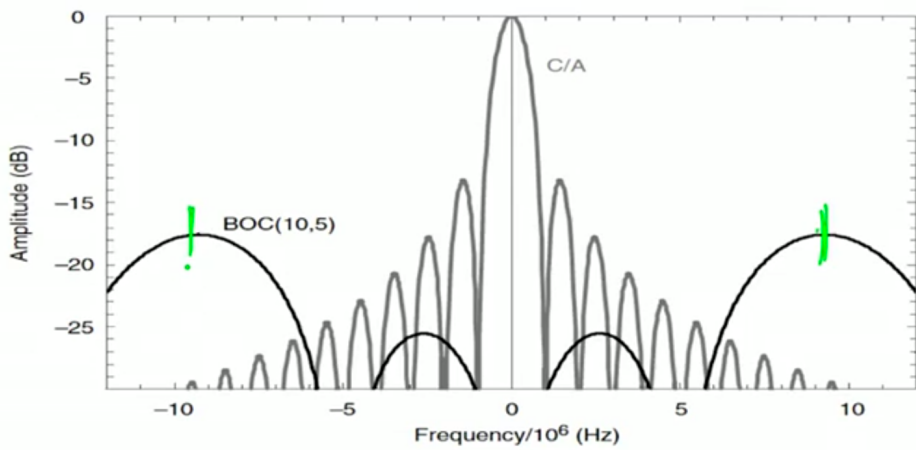
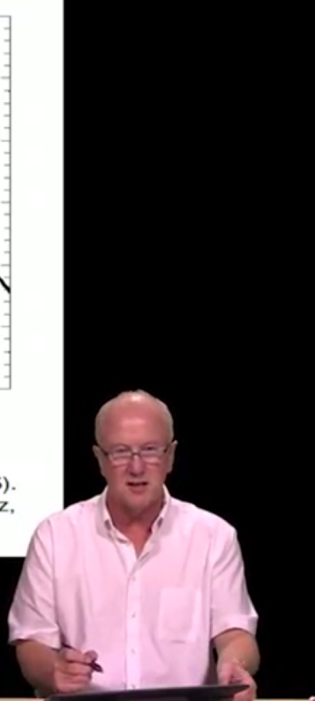
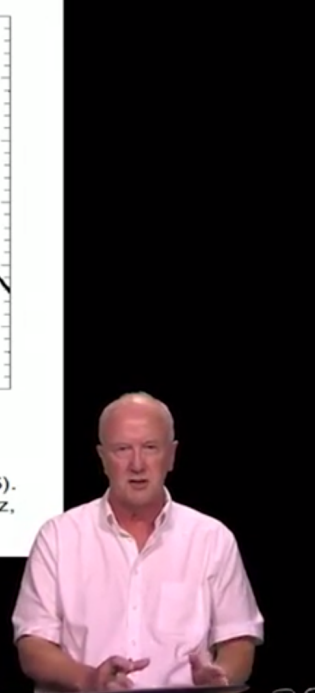
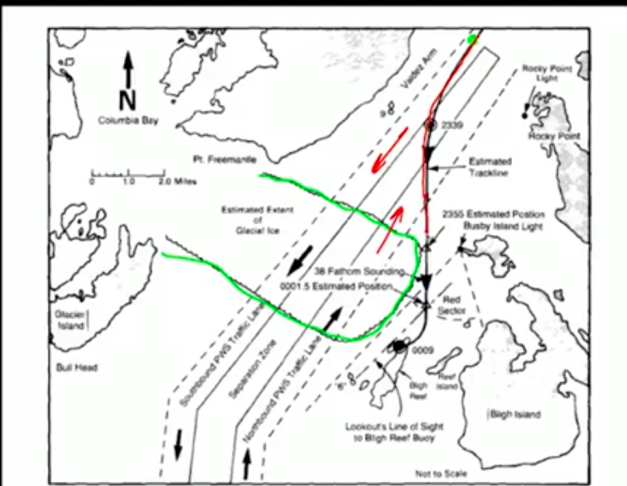


Figure 9.27 Amplitude spectrum for the C/A-code and a binary offset carrier, BOC(10,5). The BOC signal has a chipping rate of 5×10^6 and a subcarrier frequency of 10 MHz, which yields four subchips per chip ($M = 4$).



March 24, 1989

- Bound for Long Beach
- Changes course to avoid expected ice
- Grounds on Bligh Reef in Alaska's Prince William Sound
- Hull ruptures
- Spills 11 million gallons of crude oil into Prudhoe Bay
- Largest spill in U.S. coastal waters prior to the 2010 Deepwater Horizon oil spill.
- Spill impacted one thousand miles of coast.





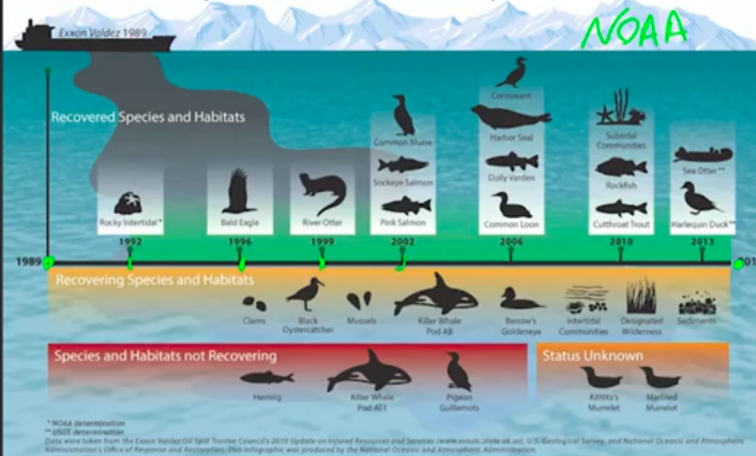
**25 YEARS
LATER**

The tanker Exxon Valdez spilled almost 11 million gallons of oil into Alaska's Prince William Sound on March 24, 1989, injuring 28 types of animals, plants, and marine habitats. How long has it taken them to recover from this spill? Twenty-five years later, which ones have not yet recovered?

Here is a timeline showing when natural resources were considered to be "recovered" by NOAA, the Exxon Valdez Oil Spill Trustee Council, and the U.S. Geological Survey. Actual recovery could have occurred earlier than presented in this timeline.



Timeline of Recovery from the Exxon Valdez Oil Spill



NOAA



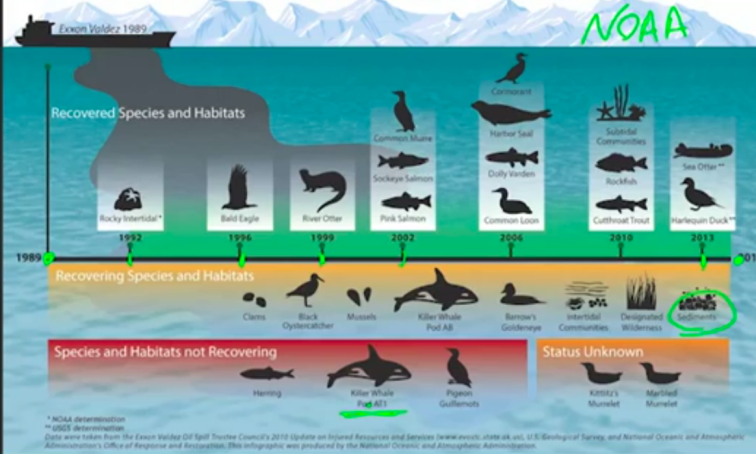
**25 YEARS
LATER**

The tanker Exxon Valdez spilled almost 11 million gallons of oil into Alaska's Prince William Sound on March 24, 1989, injuring 28 types of animals, plants, and marine habitats. How long has it taken them to recover from this spill? Twenty-five years later, which ones have not yet recovered?

Here is a timeline showing when natural resources were considered to be "recovered" by NOAA, the Exxon Valdez Oil Spill Trustee Council, and the U.S. Geological Survey. Actual recovery could have occurred earlier than presented in this timeline.



Timeline of Recovery from the Exxon Valdez Oil Spill



NOAA

